NAZARBAYEV UNIVERSITY

School of Engineering and Digital Sciences
Department of Chemical and Materials Engineering
ENG 400 Capstone Project
Course Instructor: Prof. Dhawal Shah

Design of an Industrial Plant for Production of UREA in Kazakhstan

by

Gvozdeva, Xeniya	Kabashev, Zhaksylyk	Kazhiyev, Sakengali
201943750	201824975	201994732

Kolushbayev, Aibek	Moldabekov, Kuanysh
201812416	201836507

Under the supervision of

Prof. Boris Golman and Prof. Almagul Mentbayeva

April 21, 2024

Table of Individual Contributions

Section	Xeniya	Sakengali	Aibek	Kuanysh	Zhaksylyk
Chapter 1					
Process Inroduction	2nd	1st			2nd
Chapter 2					
Material Balance		1st			
Health and Safety					1st
Chapter 3					
Reactor		1st			
Stripper			1st		
Condenser				1st	
Evaporator					1st
Prilling Tower	1st				
Chapter 4					
Carbon Dioxide Compressor	2nd	1st			
Ammonia Heat Exchanger	2nd				1st
Pumps	1st				
LPD, MPD, LPA, MPA	2nd		1st	1st	
Warehouse Storage	1st				
Chapter 5					
Plant location and layout			1st		

Continued in the next page

Section	Xeniya	Sakengali	Aibek	Kuanysh	Zhaksylyk
Chapter 6					
Environment and Wastewater					1st
Chapter 7					
Cost of Reactor		1st			
Cost of Stripper			1st		
Cost of Condenser				1st	
Cost of Evaporator					1st
Cost of Prilling Tower	1st				
Total Plant Cost			2nd	1st	
Profitablity			1st	2nd	
Chapter 8					
Conclusions and Future Work		1st			
Formatting					
All	2nd	1st	2nd	2nd	1st

Contents

List of Figures

List of Tables

Chapter 1

Process Introduction

The production of urea was estimated at 200 million tons per year globally [13]. To put it into perspective, the production capacity of sodium hydroxide (NaOH, CAS No. 1310-73-2) is only 70 million tons per year [14]. The reason for such a high demand for urea is that it is a nitrogenous fertilizer with a very high nitrogen content [15], and nitrogen is an essential element in plants' proteins, chlorophylls, and DNA [16].

The universal reaction used in urea production is Basaroff's reaction, where ammonia and carbon dioxide react to produce the ammonium carbamate intermediate (Reaction 1.1), which then disintegrates into urea and water (Reaction 1.2). The overall reaction is exothermic. The reactions occur at high temperatures and pressures. Under these conditions, the first reaction is spontaneous and happens almost instantaneously, while the second has slower kinetics [13].

$$2\,NH_{3(l)} + CO_{2(g)} \longleftrightarrow NH_2COONH_{4(aq)}, \quad \Delta H_r = -117\,kJ/mol\,CO_2 \tag{1.1}$$

$$NH_2COONH_{4(aq)} \longleftrightarrow CO(NH_2)_{2(s)} + H_2O_{(l)}, \quad \Delta H_r = +15.5\,kJ/mol \tag{1.2}$$

The two most common technologies for urea production are the Stamicarbon Avancore process and the Toyo Engineering ACES21 process. Both of them are CO2-stripping processes that use an efficient system of energy consumption and allow high-residence time for carbamate to dehydrate to urea [15, 17]. The ACES21 process is selected as a model upon which the design of the urea-production plant will be based because it results in higher CO2 conversion (60 - 63 %) [17, 18].

The reactor operates under specific conditions: a $NH_3 : CO_2$ ratio of 3.0, a temperature of 190°C, and a pressure of 175 bar. The resultant mixture includes

ammonia, carbon dioxide, ammonium carbamate, urea, and water, forming the core urea synthesis solution.

Following the synthesis, the process flow involves a CO_2 stripper, a shell and tube heat exchanger, where the remaining carbamate is decomposed back into ammonia and carbon dioxide. These are then separated from the urea and water. The bottom product from this stage is an aqueous urea solution, which is then subjected to medium-pressure decomposition and further purification.

An additional crucial component of the production process is the Vertical Sub merged Carbamate Condenser (VSCC). In the VSCC, gaseous ammonia and carbon dioxide are condensed, and the liquid carbamate obtained from the purification stage is introduced. Operating at a similar pressure but at a slightly lower temperature as compared to the stripper, the VSCC is integral in the dehydration of carbamate into urea, facilitating most of the ammonium carbamate formation.

The Process Flow Diagram of the process is depicted in Fig 1.1. As for the main units, the NH_3 input flows directly into the reactor, while the CO_2 input flows to the stripper. The two reactions occur in the reactor and the urea solution flows into the stripper, where most of the gasses are stripped off from urea and water, which then go to the medium pressure zone for purification. The gasses from the top product of the stripper proceed to VSCC, where they are condensed and react back to form ammonium carbamate. Then the solution consisting mostly of ammonia, carbon dioxide and ammonium carbamate flows to the reactor and the second-stage reaction occurs. The minor units are mostly needed for the purification of urea and for the production of commercial urea granules.

The input flow of CO_2 and NH_3 is calculated based on the required capacity of the plant. The required output annual capacity of the plant is 25% of the fertilizer demand in Central Asia. Based on analysis of the agricultural market, consumption of fertilizers, and available arable land in Uzbekistan, Turkmenistan, Tajikistan, Kyrgyzstan, and Kazakhstan, the total demand of fertilizers in Central Asia was estimated to be around 900,000 tonnes/year. Therefore, the expected capacity of the plant is 225,000 tonnes/year.

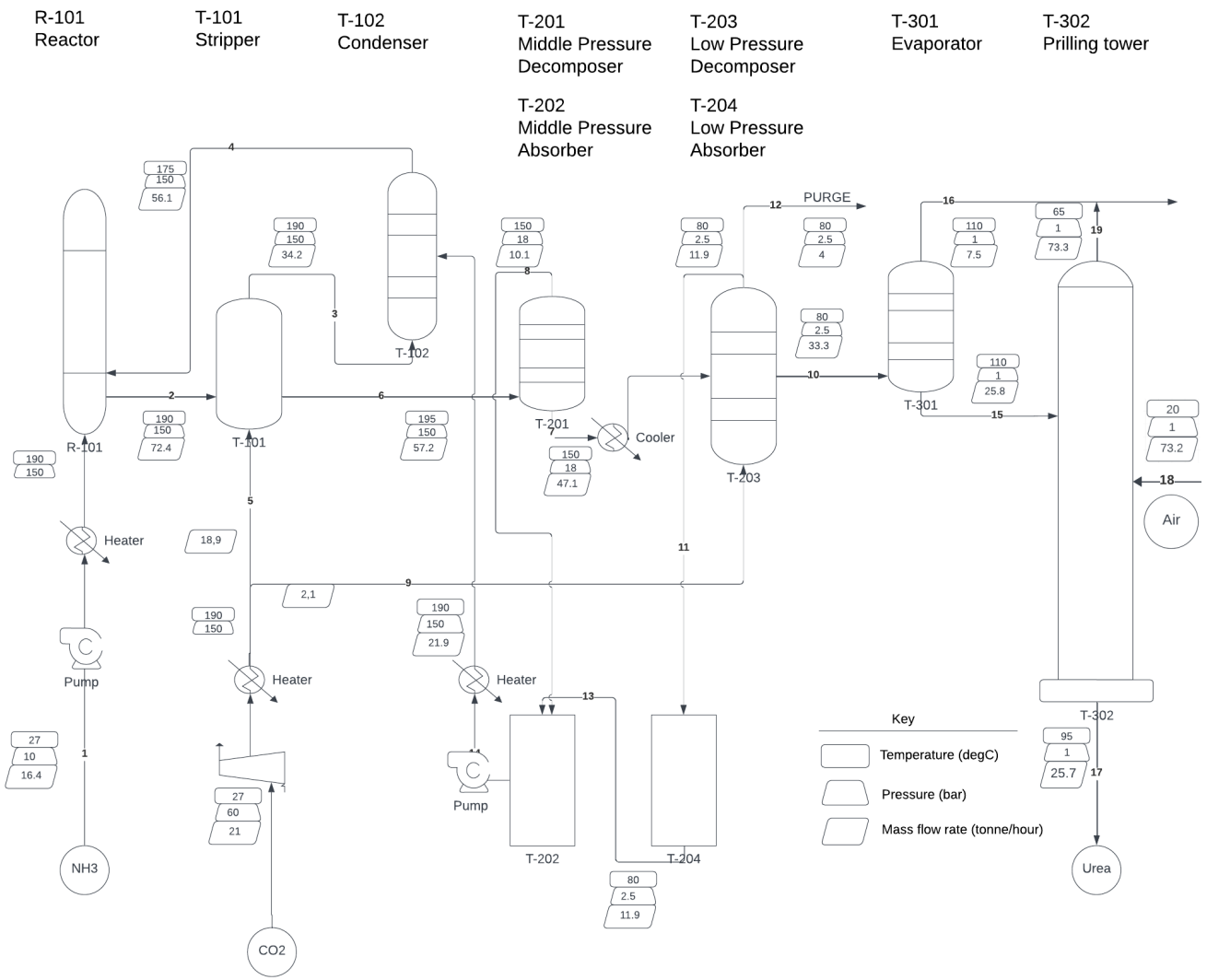

Figure 1.1: Process Flow Diagram of the process

Chapter 2

Process Summary

2.1 Material Balance

The detailed summary of the stream loads in the process, including their composition and conditions, is presented in 2.1. Conversion values of various reactions occurring in the process and split fractions in separation units are shown in Table 2.2.

Stream number	1	2	3	4	5	6	7	8	9	10	11	12	13	14	15	16	17	18	19
Temperature, °C	27	190	190	175	190	195	150	150	190	80	80	80	80	190	110	110	95	25	65
Pressure, bar	20.0	150.0	150.0	150.0	150.0	150	18	18	150.0	2.5	2.5	2.5	2.5	150.0	1.0	1.0	1.0	1.0	1.0
Vapor Fraction	0.00	0.48	1.00	0.57	1.00	0.00	0.14	1.00	1.00	0.00	1.00	1.00	0.14	0.60	0.00	1.00	0.00	1.00	1.00
Mass flow, t/h	16.4	72.4	34.2	56.1	18.9	57.2	47.1	10.1	2.1	33.3	11.9	4.0	11.9	21.9	25.8	7.5	25.7	73.2	73.3
Mole flow, kmol/h	961.5	2246.6	1262.4	1186.1	429.3	1493.9	1130.8	489.8	47.7	855.2	464.2	154.7	170.9	534.0	437.5	417.6	432.0	2524.0	2529.6
Component Flowrates, kmol/h																			
NH_3	961.5	1139.3	792.9	506.5	0.0	426.9	127.3	426.5	0.0	0.0	317.6	105.9	24.3	324.0	0.0	0.0	0.0	0.0	0.0
CO_2	0.0	0.0	469.5	164.3	429.3	0.0	0.0	63.4	47.7	0.0	146.7	48.9	0.0	0.0	0.0	0.0	0.0	0.0	0.0
NH_4COONH_2	0.0	251.4	0.0	515.2	0.0	211.2	147.8	0.0	0.0	0.0	0.0	0.0	146.7	210.0	0.0	0.0	0.0	0.0	0.0
$CO(NH_2)_2$	0.0	427.7	0.0	0.0	0.0	427.7	427.3	0.0	0.0	426.4	0.0	0.0	0.0	0.0	426.2	0.2	426.0	0.0	0.6
H_2O	0.0	428.1	0.0	0.0	0.0	428.1	428.1	0.0	0.0	428.1	0.0	0.0	0.0	0.0	10.7	417.4	5.4	0.0	5.4
$C_2H_5N_3O_2$	0.0	0.0	0.0	0.0	0.0	0.0	0.2	0.0	0.0	0.6	0.0	0.0	0.0	0.0	0.6	0.0	0.6	0.0	0.0
Air	0.0	0.0	0.0	0.0	0.0	0.0	0.0	0.0	0.0	0.0	0.0	0.0	0.0	0.0	0.0	0.0	0.0	2524.0	2524.0

Table 2.1: Material Balance of the process

Conversion values		
Condenser	CO_2 conversion to Ammonium Carbamate	0.65
Reactor	CO_2 conversion to Ammonium Carbamate	1.00
	Ammonium Carbamate conversion to Urea	0.63
Medium Pressure Decomposer	Urea conversion to Biuret	0.0001
Low Pressure Decomposer	Urea conversion to Biuret	0.0002
Fraction of decomposed Ammonium Carbamate		
Stripper	0.16	
Medium Pressure Decomposer	0.77	
Low Pressure Decomposer	1.0	
Split fractions in top product		
Stripper	NH_3	0.65
	CO_2	1.0
	Urea	0.0
	H_2O	0.0
Medium Pressure Decomposer	NH_3	0.77
	CO_2	1.0
	Urea	0.0
	H_2O	0.0
Low Pressure Decomposer	NH_3	1.0
	CO_2	1.0
	Urea	0.0
	H_2O	0.0
Evaporator	Urea	0.0005
	Water	0.975
	Biuret	0.0
Prilling Tower	Urea	0.0005
	Water	0.5
	Biuret	0.0

Table 2.2: Conversion values and split fractions in separation units

2.2 Inerts

Austenitic stainless steel, when exposed to carbamate-containing solutions used in urea synthesis, can maintain a non-corroding condition with the addition of a specific amount of oxygen. Corrosion will begin if the oxygen level falls below this threshold, with the exact timing influenced by process circumstances and the quality of the passive layer. Air is often the medium via which oxygen is delivered. Stamicarbon and Sandvik collaborated to create Safurex, a type of duplex stainless steel. Safurex has been utilised as a construction material since the 1990s, providing several notable advantages including no need for oxygen, reduced corrosion rates, resistance to stress corrosion cracking, and resistance to condensation and crevice corrosion [13].

2.3 Health and Safety

When we talk about the health and safety of industrial processes, it is important to describe it in the context of process control. To ensure safe and environmentally friendly production of urea, there is the critical role of the Hierarchy of Process Control. According to Seborg et al. [19], this hierarchy is a fundamental aspect of industrial safety and efficiency and includes layers from basic process control systems to emergency response and control. Each layer of the hierarchy plays a distinct yet interrelated role in managing operational risks, ensuring safe handling of hazardous materials, and maintaining stable process conditions. Our focus will be on understanding how safety and environmental/equipment protection layers work to create a robust and resilient safety environment in the urea production process.

Every industry, particularly those involving high temperatures, pressures, and hazardous chemicals, like fertilizer plants, has developed and adopted safety protocols [20]. These safety measures are crucial for protecting workers and minimizing risks to life and the environment. Strict adherence to these protocols is not only beneficial for individual safety but also essential for preventing broader societal and environmental impacts.

According to Mondal et al. [21], in any chemical plant, common process hazards are typically caused by various chemical reactions taking place within the processing

units. In the context of urea production, we can emphasize exothermic reactions (Bazaroff's reaction), dehydrogenation, condensation, and evaporation. Mondal et al. also describes special process hazards, which are applicable for urea production. As they point out, when storing or moving chemical materials, it is really important to be careful as these can easily leak, catch fire or explode, especially when shaken around or stored inadequately. In process units, inside and outside paints and coatings can wear off over time, or plastic and brick linings can get damaged, leading to fractures, corrosion or leaking. These are common around parts that seal or join together, especially during extreme temperatures.
To evaluate the risks and hazards during the production, the risk matrix (Figure 2.1) can be used by displaying the consequence and likelihood of identified risks [1].

		Consequence				
		Negligible 1	Minor 2	Moderate 3	Major 4	Catastrophic 5
Likelihood	5 Almost certain	Moderate 5	High 10	Extreme 15	Extreme 20	Extreme 25
	4 Likely	Moderate 4	High 8	High 12	Extreme 16	Extreme 20
	3 Possible	Low 3	Moderate 6	High 9	High 12	Extreme 15
	2 Unlikely	Low 2	Moderate 4	Moderate 6	High 8	High 10
	1 Rare	Low 1	Low 2	Low 3	Moderate 4	Moderate 5

Figure 2.1: Risk matrix [1]

A risk matrix shown in Figure 2.1 is a grid used to visually represent and assess risks in various situations. Each cell in the grid, numbered from 1 to 25, is colour-coded and categorized as low, moderate, high, or extreme risk. The x-axis represents the consequence severity ranging from negligible to catastrophic, while the y-axis indicates the likelihood of occurrence, from almost certain to rare. This tool is crucial

for understanding and managing potential hazards, particularly in the chemical industry.

High pressure processes

The high-pressure synthesis in urea plants poses significant risks, with potential ruptures in vessels, piping, and valves due to high pressure, leading to debris scattering and toxic ammonia releases [22]. Factors such as inadequate attention to piping, small diameters, and inspection challenges contribute to these dangers. Additionally, high pressure increases the corrosion rates of carbon and stainless steel by ammonium carbamate, further elevating the risk of rupture [22].

On the risk matrix, the likelihood of this happening is rare but the consequences are major, so this case falls into the moderate risk category. Thus, some actions should be taken. In the case of our plant, the materials in contact with ammonium carbamate are swapped to SAFUREX material to prevent corrosion and its consequences.

Auto-ignition of NH3 and H2

Auto-ignition of NH_3 and H_2, and air mixtures pose a significant safety risk in urea plants [23]. Given the presence of hydrogen in ammonia and carbon dioxide feeds and its increased concentration alongside oxygen during urea synthesis, there is a notable risk of explosion. Additionally, since hydrogen and oxygen dissolve in water, accumulations in plant components like ammonia-water tanks could also lead to explosions. The flammability of ammonia, combined with high temperatures used in synthesis, emphasizes the necessity of avoiding sparks, open flames, and other ignition sources in these areas [24].

On the risk matrix, the likelihood of this happening is rare but the consequences are major so this case falls into the moderate risk category. Thus, some actions should be taken. To mitigate this, it's crucial to incorporate a hydrogen removal converter in the CO_2 stream, and introduce a flash step in the NH_3 stream [24].

Crystallization

Ammonium carbamate and urea become solids at lower temperatures than the operation temperatures of a urea synthesis section. As these compounds crystallize, they cause clogging in piping and equipment limiting the blow-off capacity and causing equipment degradation [24]. On the risk matrix, the likelihood of this happening is rare and the consequences are moderate so this case falls into the low-risk category and does not require immediate prevention.

Chapter 3

Major Unit Design

3.1 Reactor

The reactor is one of the most important units in the urea production process. It has two inlets: NH_3 feed and the recycled feed from the condenser. Both of the reactions in the process, partly or completely, occur in the reactor.

3.1.1 Reactor model

The usual model for the urea reactor is a reactor with perforated plates, which is used by main industrial companies, such as Stamicarbon and TOYO [25]. These perforated plates enforce mass transfer between gas and liquid phases and prevent back-mixing. Due to independent mixing on the plates, each of them can be considered as a CSTR, therefore the whole reactor of several trays in a row can be modelled as a plug-flow reactor (PFR) [2, 26]. The reactions take place in the liquid phase (ammonia and carbon dioxide are dissolved in the solution), and for liquid phase reactors, the pressure drop is negligible [27]. Hamidipour et al. [2] modelled the urea synthesis process using these assumptions about the reactor and obtained the graph of conversion against the number of trays shown in Figure 3.1a, from which it can be inferred that the optimal number of trays in the reactor is 10. The usual height of urea reactors in the industry is 25 meters, therefore, each tray is 2.5 meters high [2]. The sketch of the suggested plate column is shown in Figure 3.1b.

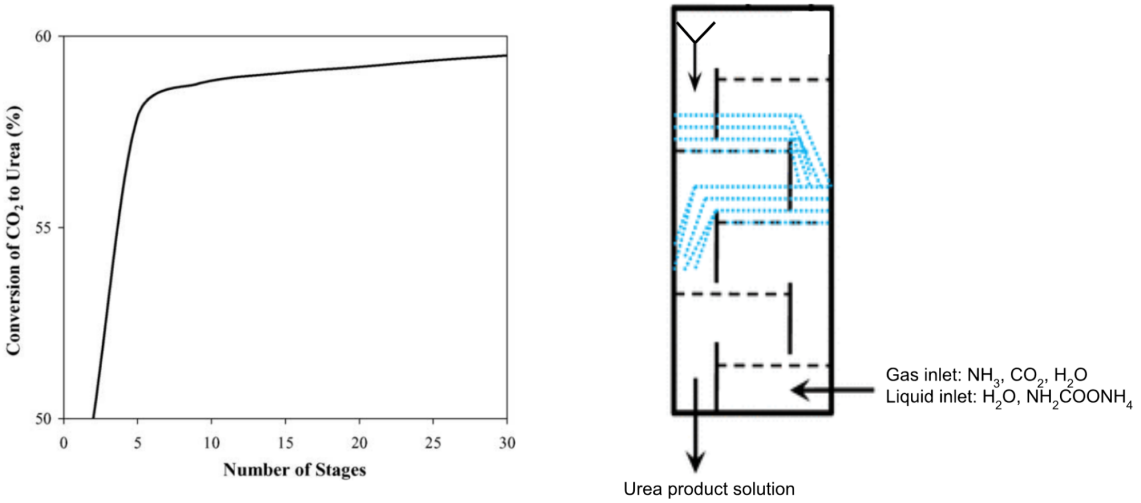

(a) (b)

Figure 3.1: (a) Conversion of CO_2 against number of trays in the urea reactor [2] (b) Scheme of the urea reactor

3.1.2 Reactor design calculations

Reaction kinetics

Reaction 1.1 is assumed to reach total completion and the kinetics of only the Reaction 1.2 is considered. In the literature, there are no kinetics that are compatible with input requirements in ASPEN simulations, therefore, here we devise our own kinetic model. The rate of the reaction is assumed to be in the form:

$$-r_A = k_1(C_{A0}(1-X))^m - k_2(C_{A0}X)^n(C_{W0}+C_{A0}X)^l \tag{3.1}$$

The experimental data for the model construction was taken from Zolotajkin et al. [28], who used a batch reactor for the reaction. Using the ideal design equation of the batch reactor:

$$t = C_{A0}\int_0^X \frac{dX}{-r_A} \tag{3.2}$$

$$t = C_{A0}\int_0^X \frac{dX}{k_1\left(C_{A0}(1-X)\right)^m - k2\left(C_{A0}X\right)^n\left(C_{W0}+C_{A0}X\right)^l} \tag{3.3}$$

Having the experimental values for time and conversion, the rate coefficients and the exponents of the components in the reaction rate equation were optimized

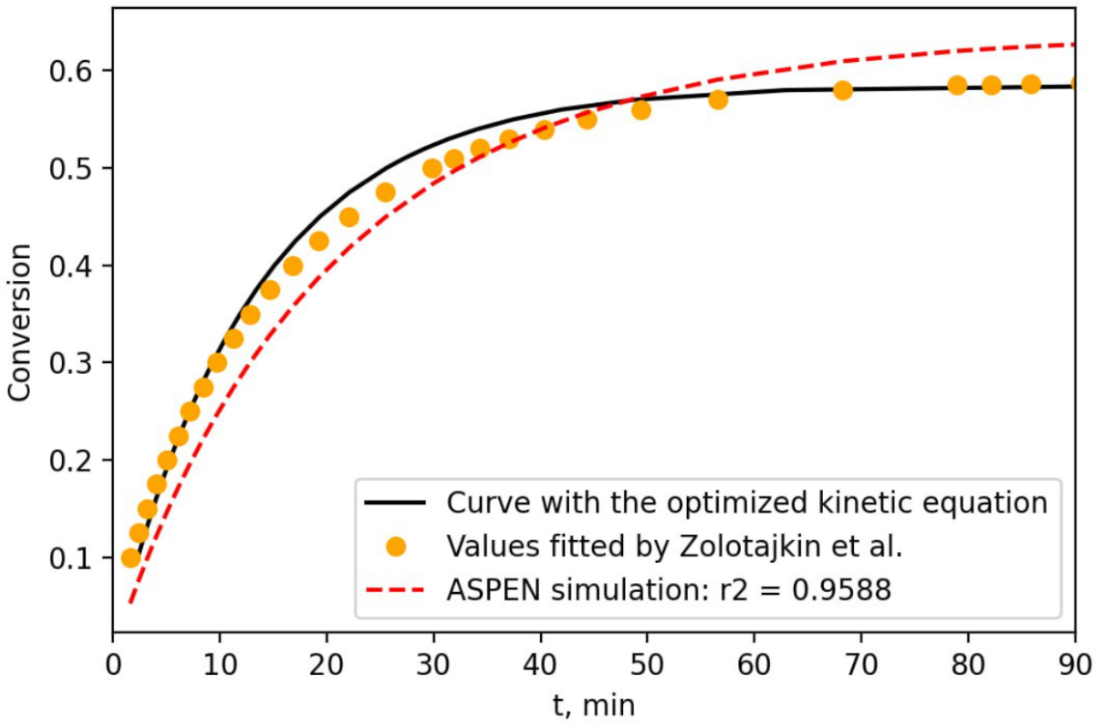

Figure 3.2: Kinetics of the reaction

using the Python Scipy Library. The optimized values are summarized in Table 3.1. The reaction kinetics was validated in ASPEN simulations and the results are shown in Figure 3.2.

$\mathbf{k_1}$	5.53e-2
$\mathbf{k_2}$	4.56e-2
m	0.7
n	1.0
l	-0.4

Table 3.1: Optimized coefficients of the kinetic equation

Heat transfer

The calculations for the heat of Ammonium Carbamate formation are shown below.

$$\Delta H_r(T) = \Delta H_r^\circ + \int_{T_1}^{T} C_p(T)\, dT \tag{3.4}$$

$$\Delta H_r = -84.03 \frac{kJ}{mol}$$

$$\dot{Q_1} = \Delta H_r \times \dot{F_{CO2}} \times X_1 = -3835kW \tag{3.5}$$

The enthalpy change of Ammonium Carbamate's decomposition to urea and water is calculated according to Equation A.7:

$$\Delta H_r = \Delta H_r^\circ + \int_{T_1}^{T} (C_{p(water)}\, dT \tag{3.6}$$

$$\Delta H_r = 27.96 \frac{kJ}{mol}$$

$$\dot{Q_2} = \Delta H_r \times (\dot{F_{CO2}} + \dot{F_{NH4CO2NH2}}) \times X = 3282kW \tag{3.7}$$

The net energy of the reactor:

$$\dot{Q}_{\text{reactor}} = \dot{Q_1} + \dot{Q_2} \tag{3.8}$$

$$\dot{Q}_{reactor} = -553kW$$

The reactions inside the reactor are overall exothermic, with a net heat duty of $-553kW$, therefore, no additional heat provision is required. Analysis of the mass transfer model for the reactor is presented in Appendix A.

3.1.3 Reactor Sizing

From the material balance of the urea process and the data from Capstone I it is known that the volumetric flow rate of the reactor inlet is 275.9 m^3/h. Since the reactor approaches PFR, the volume of the reactor is found as follows:

$$V = F_{A0} \times \int_0^X \frac{dX}{-r_A} \tag{3.9}$$

The desired conversion in the reactor is 63%, and the molar flowrate of ammonium carbamate into the reactor is 679.5 kmol/h (including the amount of carbon dioxide

that will be converted to ammonium carbamate). The volume was determined to be 298 m^3. The height of the reactor will be 25 meters, therefore, the reactor diameter will be:

$$d = \sqrt{\frac{4 \times V}{l \times \pi}} \approx 3.9 \text{ m} \tag{3.10}$$

3.1.4 Reactor details

Regarding the material of the reactor, in industry, SAFUREX is frequently used in modern urea production plants. SAFUREX is a duplex stainless steel material, developed by Stamicarbon, and is advantageous due to its high corrosion resistance [13]. The thickness of the reactor is calculated according to the following equation [4]:

$$t = \frac{P_i \times D_i}{2S - P_i} \tag{3.11}$$

The internal pressure of the reactor is 152 kPa, the internal diameter is 3.9 m, and the maximum allowable pressure of SAFUREX at 190 °C is assumed to be 104,000 kPa [4], the same as of Stainless steel, for the fact that they have a similar composition. The thickness of the reactor was found to be 5.7 mm.

3.1.5 Reactor Design Summary

Characteristics of the Urea Reactor are summarized in Table 3.2

Reactor type	Plate column
Number of trays	10
Diameter	3.9 m
Height	25 m
Height of each tray	2.5 m
Residence time	1 hour
Material	SAFUREX [13]
Reactor thickness	5.7 mm [4]

Table 3.2: Urea reactor design

3.1.6 Nomenclature

k_1, k_2 - reaction rate coefficients
C_{A0} - initial concentration of ammonium carbamate
C_{W0} - initial concentration of water
F_{A0} - initial molar flowrate of ammonium carbamate
X - conversion of ammonium carbamate
Q_0 - total volumetric inlet reactor flowrate

T - temperature
ΔH_r° - standard enthalpy change of reaction
ΔH_r - enthalpy change of reaction
C_p - constant pressure heat capacity
$\dot{F}$ - inlet molar flow rate
$\dot{Q}$ - heat flux

t - thickness of the reactor, mm
Pi - internal pressure of the reactor, Pa
Di - internal diameter of the reactor, Pa
S - maximum allowable stress for the material, Pa

3.2 Stripper

The main function of the stripping unit is to separate ammonia and ammonium carbamate from the solution with urea and water. The mixture of urea, water, ammonia and ammonium carbamate comes directly from the reactor to the top part of the stripper, and as it flows through the tubes of the stripper ammonium carbamate is decomposed. In the ACES21 process, a falling film heat exchanger is applied for stripping. In this type, the mixture flows through the tubes as a falling film on the tube walls and gasses evaporated from the surface (ammonia and carbon dioxide) flow closer to the middle of the tubes in the opposite direction [29].

Stripping units can be divided into two types: self-stripping and CO_2-striping units. The main difference is that in the second case, carbon dioxide acts as a

stripping agent and stripped components flow with carbon dioxide. During self-stripping, there is no stripping agent. In the ACES21 process, CO_2 is supplied from the bottom and acts as a stripping agent. This increases the rate and effectiveness of evaporation. Carbon dioxide supplied from the feed flows with products of ammonium carbamate decomposition (ammonia and carbon dioxide).

The heating agent used in the stripper is condensing steam at high temperature and low pressure [30]. The steam flows perpendicularly to the length of the tubes.

Due to the corrosive properties of ammonium carbamate at high temperatures in the stripper, tubes are fabricated from anti-corrosive materials, primarily from special steel grades [31]. SAFUREX was used as the tube material since it has anti-corrosive properties which eliminates the need for other corrosion protection measures.

Energy obtained from the heating agent is used to heat inlet components and ensure the decomposition of ammonium carbamate. Therefore, the conversion of ammonium carbamate depends on the steam flow rate in the shell side of the heat exchanger [32].

3.2.1 Stripper Design

Calculations of the stripping unit parameters were based on the LMTD method for a shell-and-tube heat exchanger, with the steam on the shell side and the mixture from the reactor on the tube side.

The log mean temperature difference between steam and the mixture in the tubes was calculated according to Equation 3.12.

$$\Delta T_{lm} = \frac{T_{out} - T_{in}}{ln\frac{T_s - T_{in}}{T_s - T_{out}}} \tag{3.12}$$

where $T_{in}-$ inlet temperature of the mixture , $190^{\circ}C$

$T_{\text{out}} -$ outlet temperature of the mixture, $195^{\circ}C$

T_s- temperature of the condensing steam, $225^{\circ}C$

Based on these calculations, ΔT_{lm} is equal to $32.44^{\circ}C$.

Correction factor F_t = 0.8 is assumed. The new log mean temperature difference is shown in Equation 3.13.

$$\Delta T_{lm} = 32.44^{\circ}C \times 0.8 = 25.95^{\circ}C \tag{3.13}$$

In order to calculate the surface area for the heat exchanger, Equation 3.14 took into account the heat requirement of 1.49MW, based on energy balance equations. For the purpose of calculations, the value of the heat transfer coefficient was assumed to be $750 W/m^2K$ [33].

$$A = \frac{Q}{U \times \Delta T_{lm}} = \frac{1.49MW}{750 \frac{W}{m^2 \times K} \times 25.95K} = 76.55m^2 \tag{3.14}$$

Based on these calculations, heat transfer area is equal to $76.55m^2$. Taking into account the outside diameter of 31 mm, the number of tubes is 129. With the pitch equal to 1.25×Outside Diameter, calculations of bundle diameter are shown in Equation 3.15.

$$D_b = OD_t \times (\frac{N_t}{K_1})^{\frac{1}{n_1}} \tag{3.15}$$

where D_b - bundle diameter in mm,

OD_t - tube outside diameter in mm,

N_t- number of tubes,

K_1 and $n1-$ constants.

For square pitch with 1 pass, $K_1 = 0.215$ and $n_1 = 2.207$. Therefore, the bundle diameter is equal to 563 mm.

To calculate the amount of steam condensation, the value of latent heat of vaporization of 1834.25kJ/kg of vapor was used (middle-pressure vapor at $225°C$ and vapor pressure of 25.6 bar [34]. Equation 3.16 demonstrates the calculation of steam requirements. The required mass flow of vapor is 0.81kg/s.

$$m_s = \frac{Q}{\Delta H} \tag{3.16}$$

, where Q - heat requirement of the stripper in W,

ΔH - latent heat of condensation in kJ/kg.

3.2.2 Verification of heat transfer coefficient

In order to confirm the initial assumption of the overall heat transfer coefficient U, values of heat transfer for the shell side and tube side were calculated.

Shell side

For steam at 225°C and 25.6 bar [34]:

$$\mu_l = 76.93 \times 10^{-6} Pa \times s$$

$$\rho_l = 833.57 \frac{kg}{m^3}$$

$$\rho_v = 12.806 \frac{kg}{m^3}$$

$$k_l = 0.3616 \frac{W}{m \times K}$$

For heating of the inlet mixture, vapor condenses on the shell side of the heat exchanger and moves as a condensate film on tubes outside diameter. In order to calculate heat transfer coefficient, equations for a model of condensation outside vertical tubes was applied [4].

Vertical tube loading, condensate rate per unit tube perimeter:

$$G_v = \frac{W_c}{N_t \pi D_o} = \frac{0.81 \frac{kg}{s}}{105 \times 3.14 \times 0.031 mm} = 0.079 \frac{kg}{m \times s} \tag{3.17}$$

Reynolds number:

$$Re = \frac{4G_v}{\mu_l} = \frac{4 \times 0.079 \frac{kg}{m \times s}}{76.93 \times 10^{-6} Pa \times s} = 4121 \tag{3.18}$$

Prandtl number for the condensate film is equal to 0.996, or about 1 [34].

Figure 3.3 shows the correlation between Reynolds number and condensation coefficient.

For $Re = 4121$ and $Pr_c = 1$,

$$\frac{h_c}{k_l} \left(\frac{\mu_l^2}{\rho_l (\rho_l - \rho_v) g} \right)^{1/3} = 0.128 \tag{3.19}$$

From this equation,

$$h_c = \frac{0.128 \times 0.3616 \times (833.57 \times (833.57 - 12.806) \times 9.81)}{(76.93 \times 10^{-6})^2} = 4827 \frac{W}{m^2 \times K} \tag{3.20}$$

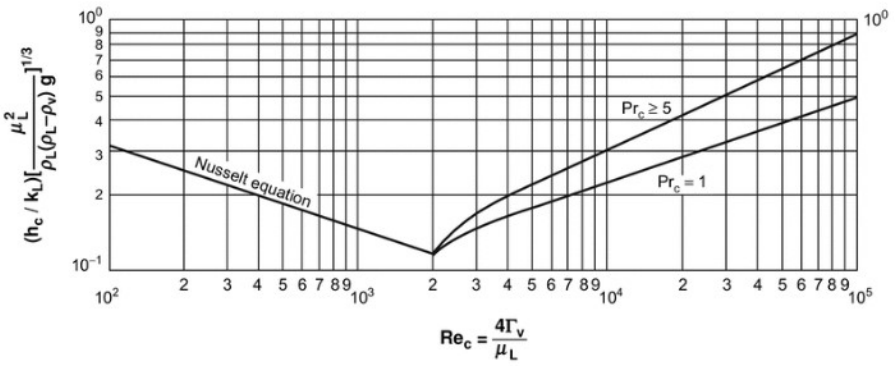

Figure 3.3: Condensation coefficient [3]

Tube side

On the tube side, there is a mixture of products coming from the reactor.
Tube cross-sectional area:

$$A_t = \frac{28^2 mm \times \pi}{4} = 615 \text{ mm}^2 \tag{3.21}$$

Number of tubes per pass:

$$N_p = \frac{129}{1} = 129 \tag{3.22}$$

Total flow area:

$$A_f = 129 \times 615 mm^2 \times 10^{-6} = 0.07939 \text{ m}^2 \tag{3.23}$$

Mass flow (from mass balance calculations):

$$\dot{m} = 20.096 \frac{kg}{s}$$

Mixture mass velocity:

$$\dot{m}_v = \frac{20.096 \frac{kg}{s}}{0.07939 m^2} = 253 \frac{kg}{s \times m^2} \tag{3.24}$$

Linear velocity:

$$u = \frac{253 \frac{kg}{s \times m^2}}{700 \frac{kg}{m^3}} = 0.361 \frac{m}{s} \tag{3.25}$$

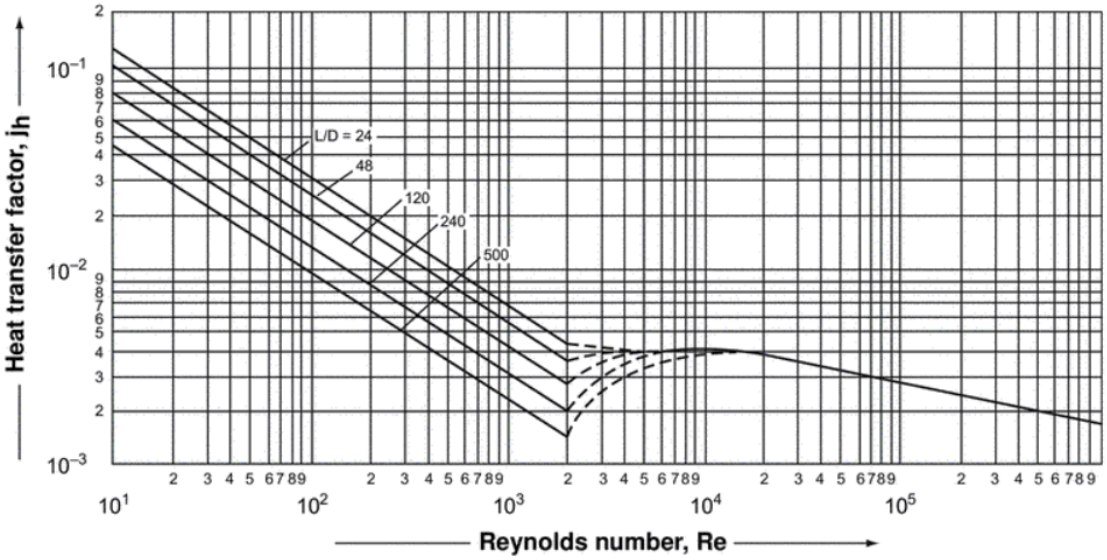

Figure 3.4: Tube side heat transfer factor [4]

Reynolds number:

$$Re = \frac{\rho u d_i}{\mu} = \frac{700\frac{kg}{m^3} \times 0.361\frac{m}{s} \times 0.028m}{0.047cP \times 10^{-3}} = 150797 \tag{3.26}$$

Prandtl number:

$$Pr = \frac{C_p \mu}{k} = \frac{1657\frac{J}{kgK} \times 0.047cP \times 10^{-3}}{0.64\frac{W}{m \times K}} = 0.121 \tag{3.27}$$

Length to diameter ratio (Tube length is 6.1m):

$$\frac{L}{d_i} = \frac{6}{0.28} = 218 \tag{3.28}$$

From Figure 3.4, j_h=0.0024

Tube side coefficient:

$$h_i = \frac{j_h Re^1 Pr^{0.33} k_f}{d_i} (\frac{\mu}{\mu_w})^{0.14} \tag{3.29}$$

$$h_i = 3544\frac{W}{m^2 K}$$

Overall coefficient

The thermal conductivity of wall material is $16W/m^2K$. The fouling coefficient for the shell side is $3000W/m^2K$. The fouling coefficient for the tube side is $5000W/m^2K$.

The overall coefficient is calculated as follows:

$$\frac{1}{U} = \frac{1}{h_o} + \frac{1}{h_{od}} + \frac{d_o ln(\frac{d_o}{d_i})}{2k_w} + \frac{d_o}{d_i} \times \frac{1}{h_{id}} + \frac{d_o}{d_i} \times \frac{1}{h_i} \tag{3.30}$$

$$U = 853 \frac{W}{m^2 \times K}$$

This confirms the initial assumption.

Tube side pressure drop:

$$\Delta P_t = N_p \times [8 \times j_f \times \frac{L}{d_i} \times (\frac{\mu}{\mu_w})^{-m} + 2.5] \times \frac{\rho \times (u_t)^2}{2} \tag{3.31}$$

For a turbulent flow, m=0.14 From [9], $j_f = 0.024$ So, $\Delta P_t = 338Pa$, which is a relatively low value, which is explained by the fact that mixture in a falling film heat exchanger flows vertically.

3.2.3 Design Summary

From the net heat duty of the stripper, surface area, number of tubes and other parameters were estimated. Calculations of heat duty and pressure drop are displayed in Appendix B. Design parameters are shown in Table 3.3.

3.3 Condenser

The VSCC, also known as the Vertical Submerged Carbamate Condenser, is located within the high-pressure section. The primary purpose of this system is to retrieve and recycle the unreacted CO2 and NH3 gases from the top part of the stripper, along with the carbamate from the bottom part of the absorption column. The system then separates the liquid phase from the gas and recycles it back to the reactor. The carbamate condenser is a two-pass heat exchanger that has a similar appearance to a kettle reboiler [35].

Type	Falling film heat exchanger
Number of tubes	129
Diameter of tubes, OD	31 mm
Diameter of tubes, ID	28 mm
Shell diameter	512 mm
Area	76.55 m^2
Length of tubes	6.10 m
Heating agent	Steam at 225°C
Material	SAFUREX stainless steel duplex

Table 3.3: Design parameters for Stripper

Ammonium carbamate, ammonia and carbon dioxide are used as a stream outside the tubes, with an inlet temperature of 190 °C and an outlet temperature of 175 °C, while maintaining a constant pressure of 150 bar. The exothermic process is utilized to heat condensed medium-pressure steam from the medium-pressure decomposer, resulting in the formation of low-pressure steam at a pressure of 4.5 bar and a temperature of 147°C. The most suitable construction materials for harsh conditions of this type are now zirconium, titanium, stainless steel duplex (SAFUREX and DP-28W), and stainless steel (25Cr-22Ni-2Mo and 316L UG) [36].

3.3.1 Calculations

Net heat duty of VSCC:

$$\dot{Q} = -11.21MW$$

Log-mean temperature difference:

$$\Delta T_{lm} = \frac{T_1 - T_2}{ln((T_1 - t_s)/(T_2 - t_s))} = 34.96^{\circ}C \tag{3.32}$$

Taking the correction factor as 0.8:

$$\Delta T_{lm} = 34.96^{\circ}C \times 0.8 = 27.97^{\circ}C \tag{3.33}$$

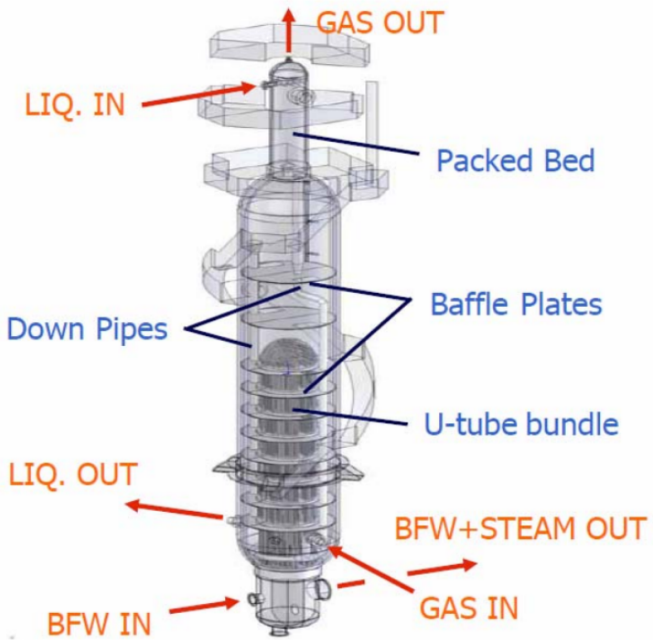

Figure 3.5: Scheme of VSCC [5]

Assuming the overall heat transfer coefficient is $750 W/(m^{2\circ}C)$, heat transfer area was calculated as follows:

$$A = \frac{11.21 MW}{750 \frac{W}{m^{2\circ}C} \times 27.97^{\circ}C} = 534.4 \text{ m}^2 \tag{3.34}$$

Assuming pipe outer diameter of 1 inch (25 mm), inner diameter 22.9mm, and length of 20 ft (6.10 m). The number of tubes in the heat exchanger was calculated with the following equation:

$$N = \frac{534.4 \text{ m}^2}{\pi \times 0.025 \text{ m} \times 6.1 \text{ m}} = 1116 \tag{3.35}$$

Hence, the tube bundle diameter with a triangular pitch with 2 passes is:

$$D_b = 0.025m \times \frac{1116}{0.249}^{1/2.207} = 1128mm \tag{3.36}$$

Bundle diametrical clearance for U type $= 19mm$
Shell diameter $= 1128 + 19 = 1147mm$

Tube-Side Coefficient

Water density from Compressed Water table at 9 bar and 147°C, ρ=920.03 kg/m^3
Water linear velocity =1.79 m/s
Viscosity of water, μ= 0.2574 cP
Thermal conductivity, $k_f = 0.6423 W/(mK)$
Water constant pressure heat capacity, $C_p = 4.1816 kJ/(kgK)$

$$Re = \frac{\rho u d_i}{\mu} = \frac{920.03 \times 1.79 \times 0.023}{0.2574} = 146510 \tag{3.37}$$

$$Pr = \frac{C_p \mu}{k_f} = \frac{4.1816 \times 0.2574}{0.6423} = 1.68 \tag{3.38}$$

$$\frac{L}{d_i} = 213 \tag{3.39}$$

From Figure 3.4,

$$J_h = 2.4 \cdot 10^{-3}$$

The tube-side heat transfer coefficient is found via the following Equation:

$$\frac{h_i d_i}{k_f} = j_h \, \mathrm{RePr}^{0.33} \left(\frac{\mu}{\mu_w} \right)^{0.14} \tag{3.40}$$

Therefore,

$$h_i = 9307.4 \ W/(m^2 K)$$

Shell-Side Coefficient

$$Re = \frac{G_s d_e}{\mu} = 89127$$

$$Pr = \frac{C_p \mu}{k_f} = 0.405$$

Taking 25% baffle cut. From Figure 3.6,

$$J_h = 0.06$$

Therefore,

$$h_s = 3418.7 W/(m^2 K)$$

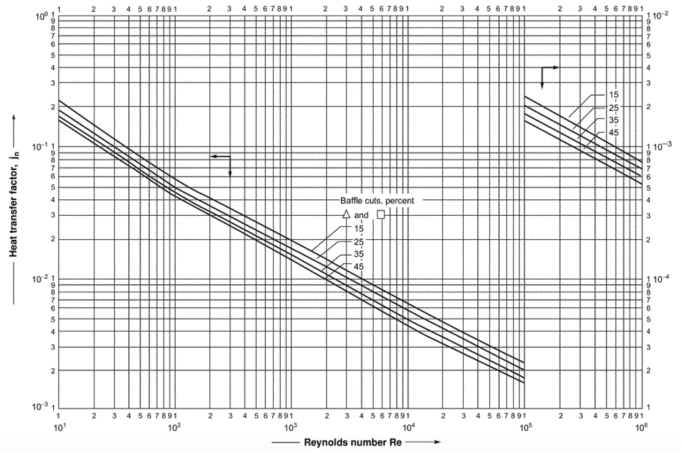

Figure 3.6: Shell-Side heat-transfer factor [4]

Overall Coefficient

The thermal conductivity of SAFUREX alloy is 16 $W/m \times K$ The fouling coefficients for the tube side is 5000 W/m^2K and the shell side is 3000 W/m^2K.

$$\frac{1}{U} = \frac{1}{h_o} + \frac{1}{h_{od}} + \frac{d_o \times ln(\frac{d_o}{d_i})}{2k_w} + \frac{d_o}{d_i} \times \frac{1}{h_{id}} + \frac{d_o}{d_i} \times \frac{1}{h_i} \tag{3.41}$$

$$U = 944 W/m^2K$$

The initial estimation of U is confirmed.

Pressure Drop

Calculations for Pressure Drop in the Shell Side are presented below:

$$Linear\ velocity = \frac{G_s}{\rho} = \frac{236}{259} = 0.911 m/s \tag{3.42}$$

From Figure 3.7, at $Re = 89127$:

$$j_f = 3.3 \times 10^{-2}$$

The viscosity correlations are neglected for the pressure drop calculations. The expression to estimate pressure drop is [4]:

$$\Delta P_s = 8 \times j_f \times (\frac{D_s}{D_e}) \times \frac{l}{l_b} \times \frac{\rho \times \mu^2}{2} \tag{3.43}$$

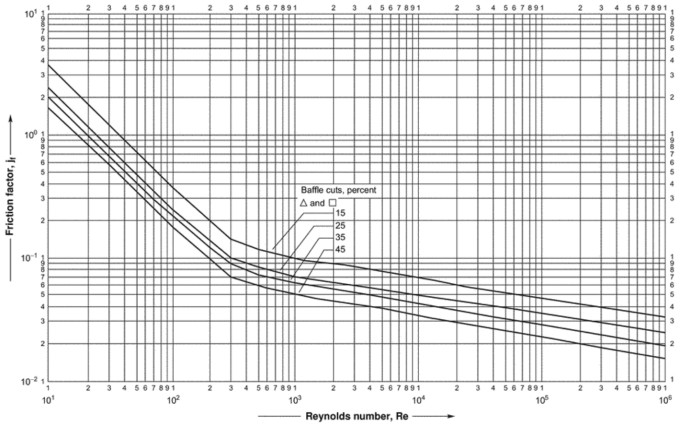

Figure 3.7: Shell-Side friction factor [4]

$$\Delta P_s = 48648 N/m^2 \approx 7 psi$$

The value of the shell-side pressure drop is $7 psi$, which is within the standard limits [4].

3.3.2 Design Summary

Net heat duty of the VSCC unit was estimated to be $-11.21 MW$ and the value was verified using Aspen simulations. Then the Tube-side and Shell-side heat transfer coefficients were calculated, and then the overall heat transfer coefficient and the heat transfer area were estimated. Based on theses values, the major design parameters for VSCC were determined. All the calculations are presented in Appendix C. The design parameters for VSCC are summarized in Table 3.4.

Type	Vertical shell-and-tube type heat exchanger
Number of tubes	1116
Diameter of tubes, OD	25 mm
Diameter of tubes, ID	22.9 mm
Shell diameter	1147 mm
Area	534.4 m^2
Length of tubes	6.10 m
Cooling agent	Water at 147°C
Material	SAFUREX stainless steel duplex

Table 3.4: Design parameters for VSCC

3.4 Evaporator

3.4.1 Evaporation unit overview

In the urea production, an evaporator unit is used to concentrate and purify the final product. The liquid urea solution with impurities (less than 1% of biuret, ammonia, carbon dioxide) from the low pressure decomposer is fed into an evaporator which consists of several sections that yield high purity (99%) urea melt. In short, the evaporator unit has two outlets: urea-water mixture is fed to the evaporator unit where water is evaporated and urea melt is sent further to the prilling tower. In turn, evaporated water (containing some impurities in the form of residual urea and biuret) is sent to the water treatment unit.

To effectively concentrate the urea solution while minimizing side reactions such as biuret formation and hydrolysis, the evaporation process is conducted under vacuum conditions [13, 37].

Sergeev et al. [38] report that film-type heat exchangers are used in the evaporation process of urea solutions. These film-type vacuum evaporators (the liquid product falls as a thin film on the tubes while being evaporated) are distinguished by their enhanced efficiency in heat exchange. A notable advantage of this design is the reduced residence time of the urea solution within the evaporator, which is crucial in minimizing the formation of biuret [38, 39].

The schematics of the evaporator unit and the falling film evaporation are given in figure 3.8a.

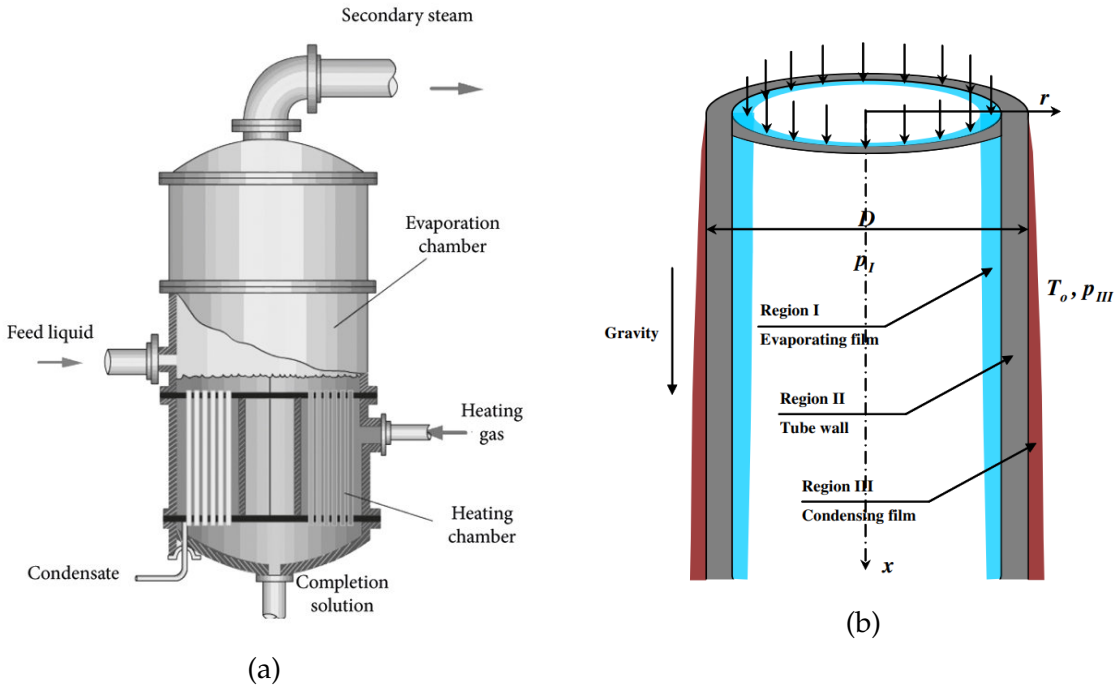

Figure 3.8: Schematics of (a) the vacuum evaporator [6] and (b) internal evaporation and external condensation films in the tubes [7]

As shown in figure 3.8b, the urea-water liquid feed is distributed at the top and flows downward over the inner surfaces of vertically aligned tubes. As the liquid descends, it forms a thin film along the tube walls, which enhances heat transfer efficiency.

The heating steam, circulates outside the tubes, transferring heat to the film and causing the water to evaporate. The resulting vapor is then collected and separated from the concentrated liquid. Falling film evaporators are known for their high heat transfer rates, low retention time, and efficient use of energy.

3.4.2 Evaporation unit design

All detailed calculations are given in the Appendix D.

Streams and Components:

Evaporator inlet (from LPD) is mostly urea, water and unreacted biuret (liquid). The evaporator has two outlets: outlet 1 (to waste water) is mostly water and residual urea (liquid) and outlet 2 (to the prilling tower) is 99% urea melt and negligible water and biuret. The evaporator pressure is reduced to 1 atm and the outlet stream temperature is set to 110 °C. The total energy required to evaporate 428.11 kmol/h of water is $5.4MW$ (Appendix D).

Component	Boiling Temp, K	Specific heat, kJ/kmol	Latent heat of vaporization, kJ/mol	Inlet molar flowrate, kmol/h	Mole frac
Urea	421.21	94.00	45.85	426.40	0.498
Water (l)	373.15	75.32	40.65	428.11	0.501
Steam	–	37.47	–	–	–
Biuret	669.79	131.30	70.52	0.64	0.001

Table 3.5: Evaporator components thermochemistry

Evaporator Design:

To design a falling-film evaporator, we use a method suggested by Fang et al. [40] and Kern's model (described in [9]). According to Sinnott & Towler [9], for the vaporizers using steam and aqueous solutions (because our process involves heating a water-based solution to cause evaporation), the overall heat transfer coefficient, U, is in the range 1000–1500 W/m^2K. The steam is a corrosive fluid, thus steam will go to the shell side.

Let the first assumption for U be $1500W/m^2K$. Area of the heat-exchanger, A is given by:

$$A = \frac{\dot{Q}}{U \times \Delta T_{lm}} \tag{3.44}$$

Where U is the overall heat transfer coefficient and ΔT_{lm} is log mean temperature, 33.66 $^\circ C$.

$$A = 106.8m^2$$

Assume tubes with 5cm diameter and 150cm length. The number of tubes, n :

$$n = 454$$

Heat transfer outside the tubes:

According to Fang et al. [40], Reynolds number for thin film flow is:

$$Re = \frac{4\Gamma}{\mu} = \frac{4 \times 67.54/(454 \times 2 \times \pi \times 0.025)}{0.28} = 13.53 \tag{3.45}$$

Where Γ is the wetting rate (mass flow rate per unit circumference) in $kg/m \times s$ and μ is the dynamic viscosity in $kg/m \times s$.

$$Pr = \frac{C_p \mu}{k} = \frac{4181 \times 0.28}{0.677} = 1729 \tag{3.46}$$

Where k is thermal conductivity. According to Sinnott & Towler [9], total heat transfer coefficient at the outside (U_o) is equal to:

$$U_o = \frac{k}{D} Re^1 Pr^{0.33} = \frac{0.677}{0.050} \times 13.53 \times 1729^{0.33} = 2199 W/m^2 K \tag{3.47}$$

Tube side heat coefficient:

Cross sectional area =

$$\frac{\pi}{4} \times D^2 = 1963 mm^2$$

Number of tubes = 454
The total flow area = $454 \times 1963 \times 10^{-6} = 0.89 m^2$
Urea-water mixture mass flow rate= 9.25 kg/s

$$\rho_{mixture} = \frac{m_1 \rho_1 + m_2 \rho_2}{m_{total}} = \frac{7.11 \times 1320 + 2.14 \times 998}{9.25} = 1245 kg/m \tag{3.48}$$

Mixture viscosity:

$$\frac{1.0 + 1.4}{2} mPa \times s = 1.201 mPa \times s \tag{3.49}$$

Mixture heat capacity:

$$1.56 \times 0.498 + 4.18 \times 0.501 = 2.87 kJ/kgK$$

Thermal conductivity of the mixture[41]:

$$(0.0265 + 0.673)/2 = 0.350 W/m.K$$

Tube inner radius = 0.022m[41]

$$Re = \frac{4\Gamma}{\mu} = \frac{4 \times 9.25/(454 \times 2 \times \pi \times 0.022)}{1.201} = 0.49$$

$$Pr = \frac{C_p \mu}{k} = \frac{2870 \times 1.201}{0.35} = 9848$$

According to Fand et al.[40], heat transfer coefficient for the laminar falling film fluid is given by

$$U_i = 62.09 Re^{-0.01239} Pr^{0.3427} \tag{3.50}$$

$$U_i = 62.09 \times 0.49^{-0.01239} \times 9848^{0.3427} = 1463 W/m^2 K$$

Total heat coefficient:

According to Fang et al.[40], the total heat coefficient U_t for the thin film evaporator is given by:

$$\frac{1}{U_t} = \frac{1}{h_o} + \frac{d_t}{k_w} + \frac{\delta}{h_i} \tag{3.51}$$

Where d_t is tube thickness, h_o and h_i are heat transfer coefficients outside and inside of the tube (respectively), and δ is the falling film thickness.
Assume film thickness of 1 mm and the stainless steel material with $k_w = 15 W/m.K$. Sinnott and Towler [9] report that the appropriate tube thickness for a 50mm outer diameter tube is 2.8mm.

$$\frac{1}{U_t} = \frac{1}{2199} + \frac{2.8 \times 10^{-3}}{15} + \frac{1 \times 10^{-3}}{1463} \tag{3.52}$$

$$U = 1557 W/m^2 K$$

Total heat coefficient U was calculated to be $1557 W/m^2 K$ which is pretty close to the assumed $1500 W/m^2 K$.

The consistency between the assumed and calculated overall heat transfer coefficients validates the accuracy of the initial design assumptions and confirms the robustness of the heat transfer analysis conducted. It suggests that the selected specifications are well-aligned with the operational requirements.
The evaporator results were also validated in Aspen Plus.

Pressure drop

The pressure drop calculations for falling-film evaporator is unusual. The liquid film flows downwards under gravity, while being evaporated.

The pressure drop Δp in the tubes of a falling-film evaporator can be estimated using the Hagen-Poiseuille Equation for laminar flow in pipes. For simplicity, we assume that the liquid components move at the same velocity and the liquid has uniform properties.

$$\Delta p = \frac{8\mu LQ}{\pi R^4} = \frac{8 \times 1.201 \times 1.5 \times 1.64 \times 10^5}{\pi \times 0.025^4} = 193Pa \tag{3.53}$$

In falling film evaporators, the pressure drop is generally very low due to the nature of the flow, where the fluid travels down the inner surface of the tubes or plates under gravity with minimal resistance.

The design characteristics of the evaporator are summarized in Table 3.6, and the detailed calculations can be found in Appendix D.

Evaporator type	Falling-film
Heat transfer area	106.8 m^2
Number of tubes	454
Diameter of one tube	5 cm
Tube length	1.5 m
Tube thickness	2.8 mm
Material	Stainless Steel

Table 3.6: Evaporator design summary

3.5 Prilling tower

Prilling is a major granulation process in which a highly concentrated solution or melt is sprayed in droplet forms, and allowed to fall through a gaseous cooling medium and solidify to become granular particles called prills [42]. As a result of prilling, approximately ideal spherical particles are made with almost uniform size distribution. The schematic of the prilling tower is presented in Figure 3.9. The design characteristics of the prilling tower are summarized in Table 3.7, and the appropriate calculations can be found in Appendix 3.6.

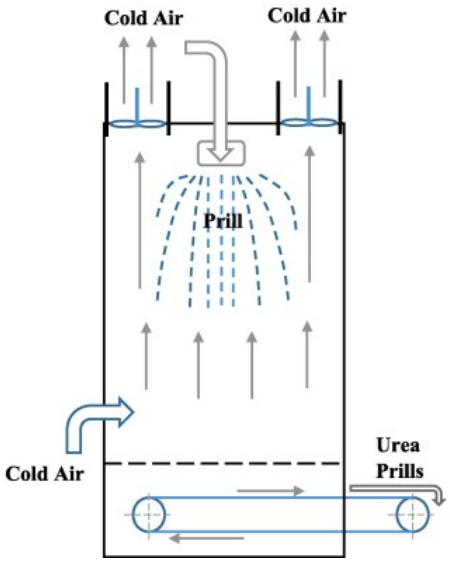

Figure 3.9: Schematic representation of a prilling tower used for urea production

Number of holes in a sprayer, no unit	2500	Diameter of a prill, mm	1.9
Heat transfer coefficient, W/m^2K	830	Time for a droplet to solidify, s	1.93
Height of the tower, m	74	Diameter of a sprayer, m	2.8

Table 3.7: The design characteristics of a prilling tower used for urea production

3.6 Prilling Tower Design Calculations

To design the prilling tower, the properties and their values are listed in Table 3.8.

Pr	0.72	k_a	$0.026 \frac{\mathrm{W}}{\mathrm{mK}}$
P_1	60 psi (4.14 bar)	ΔH_{fus}	$233100 \frac{\mathrm{J}}{\mathrm{kg}}$
P_2	1 bar	Air T	$20^{\circ}\mathrm{C} = 293$ K[43]
$\rho_{\mathrm{urea},s}$	$1335 \mathrm{m}^3$[44]	T_m	406 K
$\rho_{\mathrm{urea},l}$	$750 \frac{\mathrm{kg}}{\mathrm{m}^3}$[44]	k_{urea}	$0.55 \frac{\mathrm{W}}{\mathrm{mK}}$
μ_{urea}	1.410^{-3} Pa[45]	σ_{urea}	$0.0755 \frac{\mathrm{N}}{\mathrm{m}}$[45]
C_p	$1.01 \frac{\mathrm{J}}{\mathrm{kgK}}$[46]		

Table 3.8: Input parameters for Prilling Tower design

Pr - Prandtl number, P - pressure (subscript 1 means in the nozzle, 2 - in the prilling tower). ρ - density (subscript s means solid, l - liquid), μ - viscosity, k - thermal conductivity (subscript a means air), H - latent heat of solidification, T-temperature (Tm - melting temperature of urea), σ - surface tension, Cp - heat capacity of air.

Further in the equations, the following symbols are used, which are calculated based on quantities in Table 3.8: Re_h - Reynolds number based on hydraulic head, dimensionless; d - nozzle diameter, m; v_0 - velocity of the urea droplet, m/s; M - total mass flow rate in the nozzle, kg/h; C_d - discharge coefficient, dimensionless; C_{dU} - ultimate discharge coefficient, dimensionless; $\frac{L}{d}$ - length of nozzle to nozzle diameter ratio, dimensionless; A - cross-sectional area of nozzle, m^2; λ_{opt} - wavelength of the liquid column at the optimum perturbation, m; R - radius of droplet, m; h - heat transfer coefficient, kW/m^2K.

Prandtl number is calculated as follows [46]:

$$\mathrm{Pr} = \frac{C_p \mu_a}{k_a} \tag{3.54}$$

Reynolds number is based on hydraulic head and calculated as follows [47]:

$$\mathrm{Re}_h = \frac{d \rho_{\mathrm{urea}}}{\mu_{\mathrm{urea}}} \sqrt{\frac{2\left(P_1 - P_2\right)}{\rho_{\mathrm{urea}}}} \tag{3.55}$$

$$v_0 = \sqrt{\frac{2\left(P_1 - P_2\right)}{\rho_{\text{urea}}}} = \sqrt{\frac{2(4.14-1)10^5}{750}} = 28.9\frac{\text{m}}{\text{s}} \tag{3.56}$$

:

$$C_{dU} = 0.827 - 0.0085 L/d = 0.62 \tag{3.57}$$

From [44]:

$$L/d = 24.35 \tag{3.58}$$

$$C_d = \frac{1}{\frac{1}{C_{dU}} + 20\frac{(1+2.25L/d)}{Re_h}} \tag{3.59}$$

Mass flow rate of the nozzle:

$$M = C_d A \sqrt{2\rho_l (P1 - P2)} \tag{3.60}$$

Overall mass flow rate in the prilling tower, based on mass balance, equals 25.8 ton/h. If we assume 2500 holes, then mass flow rate over each opening in the nozzle will be $\frac{25.8}{2500} = 10.36$ kg/h.

As the main constants are known, based on the equations above, Reynolds number, C_d and mass flow rate over one opening are presented as functions of nozzle diameter.

Based on Saleh et al. [47]:

$$Re_h = \frac{d750}{1.410^{-3}} \sqrt{\frac{2(4.14-1)10^5}{750}} = 15.5010^6 \text{ d} \tag{3.61}$$

From Skydanenko et al. [48]:

$$\begin{aligned} C_d &= \frac{1}{\frac{1}{0.62} + 20\frac{(1+2.25L/d)}{15.50\cdot 10^6 d}} = \frac{1}{1.613 + \frac{1.29010^{-6}}{d} + 2.90310^{-6}\frac{L/d}{d}} \\ &= \frac{d}{1.613d + 1.29010^{-6} + 2.90310^{-6}\frac{L/d}{d}} \end{aligned} \tag{3.62}$$

From Halonen et al. [45]:

$$\begin{aligned} M &= C_d \frac{\pi d^2}{4} \sqrt{2\rho(p1 - p2)} \\ &= \frac{\pi d^3}{6.452d + 5.16010^{-6} + 11.61210^{-6}\frac{L/d}{d}} \cdot \sqrt{2 \cdot 750(4.14-1)10^5} \\ &= \frac{21703\pi d^3}{6.452d + 5.16010^{-6} + 11.61210^{-6}\frac{L/d}{d}} \\ &= 10.36\frac{\text{kg}}{\text{h}} = 0.00288\frac{\text{kg}}{\text{s}} \end{aligned} \tag{3.63}$$

Using Newton-Raphson method, the values shown in Table 3.9 were obtained. The wavelength of the liquid column at the optimum perturbation is calculated as

d, mm	1.9
Mass flow rate over 1 nozzle, M, $\frac{kg}{s}$	0.02874

Table 3.9: The nozzle diameter and corresponding mass flow rate over a single nozzle obtained based on 3.63 and Newton-Raphson method.

follows:

$$\lambda_{\text{opt}} = \sqrt{2\pi} d \left(1 + \frac{3\mu}{\sqrt{\rho_l \sigma d}}\right)^{0.5} \tag{3.64}$$

$$\lambda_{\text{opt}} = \sqrt{2\pi} \times 0.0019 * \left(1 + \frac{3 \times 1.410^{-3}}{\sqrt{750 \times 0.0755 \times 0.0019}}\right)^{0.5} = 0.00478 \text{ m}$$

Diameter of the droplet is calculated as follows:

$$D = \left(1.5 \lambda_{\text{opt}} d^2\right)^{\frac{1}{3}} \tag{3.65}$$

$$D = \left(1.5 \times 0.00478 \times 0.0019^2\right)^{\frac{1}{3}} = 0.00295 \text{ m}$$

The Ranz-Marshall correlation is used to determine heat transfer coefficient:

$$Re_h = 15.50 \times 10^6 \times 0.0019 = 29374 \tag{3.66}$$

$$h = \frac{k_a}{D}\left(2 + 0.6 \,\text{Re}^{0.5} \,\text{Pr}^{0.33}\right) \tag{3.67}$$

$$h = 830.0 \frac{W}{m^2 K}$$

Time required for a droplet of urea to solidify [47]:

$$t_s = \frac{\rho \Delta H_s R}{h\left(T_m - T_a\right)}\left[\frac{1}{3} + \frac{1}{6}\frac{hR}{k}\right] \tag{3.68}$$

$$t_s = \frac{750 \times 233100 \times 0.00295}{830 \times (406 - 293) \times 2}\left(\frac{1}{3} + \frac{1}{6} \times \frac{830 \times 0.00295}{2 \times 0.55}\right) = 1.93 \text{ s}$$

The required height of the column is calculated via free fall equation:

$$H = v_0 \times t + \frac{1}{2} \times g \times t^2 \tag{3.69}$$

$$H = 28.9 \times 1.93 + \frac{1}{2} \times 9.81 \times 1.93^2 = 74 \text{ m}$$

When the height of the prilling tower for smaller diameter prills equals 45 m, the temperature in the lower part of the tower, based on plant data [49], almost reaches the inlet air temperature. We assume that as the tower is taller, the outlet temperature will be even closer to the inlet air one. Thus, we assume the temperature at the lower part of the tower to be $35°C$, 308 K. We also assume that the inlet air is dry and does not contain water. Air velocity is assumed to be 2.5 m/s, and the diameter able to accommodate 2500 total number of orifices in the upper part of the spray part of the tower is assumed to be 2.8 m, which corresponds to the diameter of the tower taken for CFD simulations for prilling tower design for urea production [47]. Based on these, the mass and molar flow rates of inlet air are calculated as follows:

$$m_{air} = v_{air} \times \rho_{air} \times A_{tower} \tag{3.70}$$

$$m_{air} = \frac{2.5 \times 3600 \times 1.3 \times \pi \times 2.8^2}{4} = 73196 \frac{\text{kg}}{\text{h}} \tag{3.71}$$

$$\omega_{air} = \frac{m_{air}}{M_{air}} \tag{3.72}$$

$$\omega_{air} = \frac{73196}{29} = 2524 \frac{\text{kmol}}{\text{h}} \tag{3.73}$$

m_{air} – mass flow rate of air, kg/m^3; v_{air} – velocity of air, m/s; A_{tower} –cross-sectional area of prilling tower, m^2 ; ω_{air} - molar flow rate of air, $kmol/h$; M_{air} –molar mass of air, g/mol.

The outlet air temperature estimation is based on air and urea mass flow rates and assumed equivalence of heat flow rates of urea cooling and air heating as follows. The heat capacity of urea, C_{urea} equals 122 $J/molK$ [50], and C_{air} equals 34.3 $J/molK$ [51]:

$$\Delta T_{air} = \frac{426.2 \times 122 \times (383 - 308)}{73196 \times 34.3} = 45 \text{ K} \tag{3.74}$$

Meaning that the outlet air temperature equals 338 K.

Chapter 4

Minor Units Design

4.1 Carbon Dioxide Compressor

The compressor is required to compress the input CO_2 inlet to the required reaction pressure of 150 bar. The appropriate compressor type is Reciprocating Compressor, a subtype of Positive Displacement Compressors. The drawing of Reciprocating Compressor is shown in Figure 4.1.

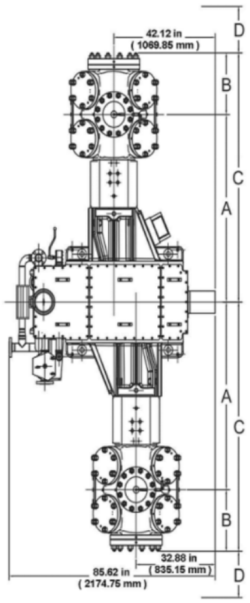

Figure 4.1: Dimensions of the reciprocating compressor for the process [8]

Characteristics of the CO2 compressor used in urea production are summarized in Table 4.1.

Cylinder Size, mm	228.6	Maximum allowable operating pressure, bar	165.5
A, mm	1619	Number of cylinders, no unit	6
B, mm	486	Nominal Power, kW	5816
C, mm	2108	Maximum Allowable Gas Load, ton	40
D, mm	1041	Rated Rotations Per Minute (RPM)	1000

Table 4.1: Dimensions and operating characteristics of the CO2 compressor

4.2 Pumps

Two main pumps are considered: for pure ammonia flowing into the reactor and for ammonia - ammonium carbamate mixture in Stream 14 on the PFD. The summary of the characteristics for both pumps are collected in Table 4.2, and the schematics of the pumps are presented in Figures 4.3 and 4.2. The first pump is chosen to be a standard XCN Close Coupled Centrifugal [10] pump made of Duplex, and the second one is Reda® Schlumberger™ GN7000 [52] accounting for a multiphase flow.

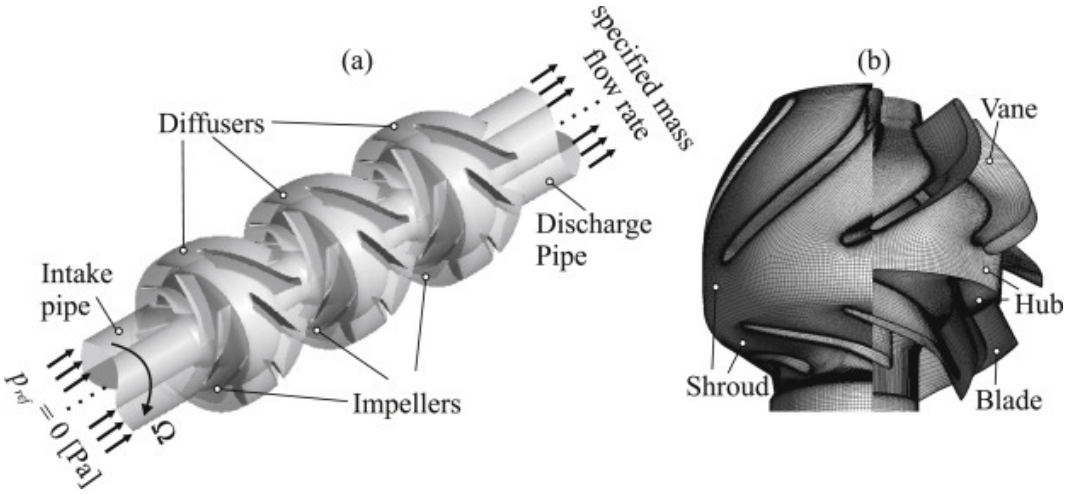

Figure 4.2: The schematics showing the internals of the multiphase pump the Reda® Schlumberger™ GN7000

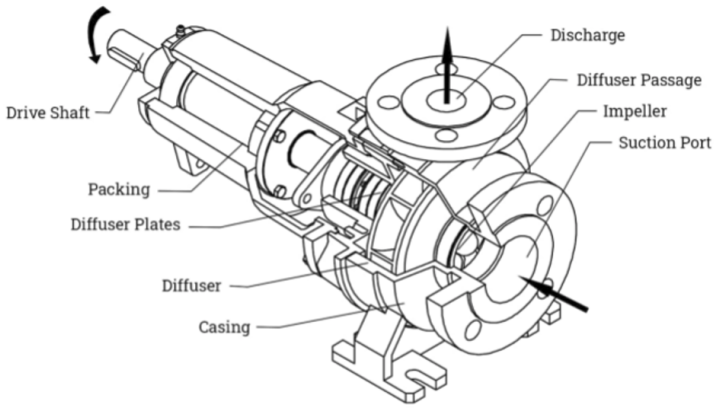

Figure 4.3: The main components of a centrifugal pump

Pump	Inlet size, mm	Outlet size, mm	Efficiency, %	Hydraulic head, m
XCN Close Coupled Centrifugal	32	150	70	152
Reda® Schlumberger™ GN7000	30	83	67	9.6

Table 4.2: The pump characteristics for urea production plant [10]

4.3 Heater Exchanger

Before ammonia enters the reactor, it is preheated from 27°C to 190°C using a shell and tube heat exchanger made of copper-brass alloy [53]. The hot steam flows within the shell transferring heat to the cooler ammonia flowing through the tubes. The schematics of the heat exchanger are shown in figure 4.4.

The summary of design characteristics for the heat exchanger is presented in Table 4.3.

4.4 Low Pressure and Medium Pressure Decomposers and Absorbers

Both decomposers are falling-film heat exchangers [54] with square pitch and one pass. The design characteristics of the low pressure (LP) and medium pressure

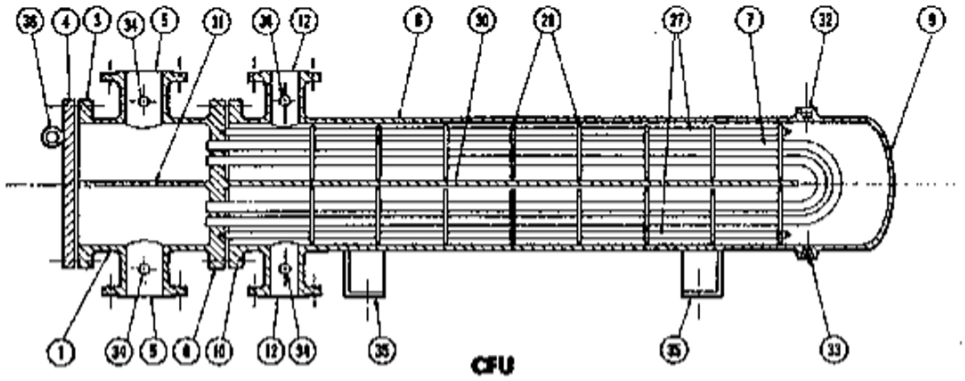

Figure 4.4: The shell and tube heat exchanger schematics [9]

Shell diameter, mm	411	Number of tubes, no unit	132
Shell Tm, °C	29.5	Outside tube diameter, mm	20
Area, m^2	40.04	Inside tube diameter, mm	16
Heat transfer coefficient h on shell side, W/m^2K	8146	Length of a tube, m	4.83
Heat transfer coefficient h on tube side, W/m^2K	2617	Bundle diameter, mm	343
Overall heat coefficient U, W/m^2K	1912	Tubes per pass, no unit	66

Table 4.3: Design characteristics of the heat exchanger for ammonia pre-heating

(MP) decomposers and absorbers are presented in Table 4.4. The calculations are presented in Appendix.

4.5 Warehouse Urea Bags Storage

Raw materials flowing in the reactor are ammonia and carbon dioxide, for continuous flow of which the pipes are used, so no storage site is required for initial reactants. As for the main product, urea in prilled form, storage is needed.

As prills are formed in the prilling tower, the prills flow out of the tower to bagging in the warehouse using a conveyor belt and are left in a storage part of the warehouse for which the design is considered in this subchapter. The prills are very sensitive to moisture, which is why the final product should be stored and

Equipment	Area, m^2	Number of tubes, no unit	Bundle diameter, mm	Steam mass flow rate, kgs
LP Decomposer	222	381	919	13.63
MP Decomposer	295	505	1044	5.90
LP Absorber	355	740	1001	31.58
MP Absorber	184	384	744	18.93

Table 4.4: Low pressure and medium pressure decomposers' and absorbers design characteristics

Bag volume, m^3	1 [56]	Storage temperature, $°C$	20
Bag mass, kg	1000 [56]	Width of the storage, m	22
Package material	Opaque polypropylene [57]	Length of the storage, m	181
Number of bags stored in 1 week, unit-less	5250	Height of the storage, m	10

Table 4.5: Design characteristics related to the urea bags storage

delivered in dry and dark conditions at temperatures between 5 to 30°[55]. The assumption is that the prills will be delivered out of the plant to the market once a week. The characteristics of the bags together with the dimensions of the storage room based on calculations shown in the Appendix are summarized in Table 4.5.

Chapter 5

Plant Location and Layout

5.1 Plant Location

The choice of location for the production unit was made based on the availability of feedstock, workforce, basic utilities (water, electricity, heat) and transportation infrastructure (railways and roads). Another consideration is the transportation of the final product and proximity to the market.

The two main types of feedstock in the process are ammonia and carbon dioxide. While ammonia can be transported on railways or via an ammonia pipeline, carbon dioxide is mainly transported in balloons that can be transported either on railways or automobile roads. Alternatively, carbon dioxide can be transported in pipeline for short distances. The only producer of ammonia in Kazakhstan is KazAzot, whose plant is located in Aktau city. The production capacity of ammonium is about 200,000 tons per year [58]. There are also large producers of ammonia in Russia, including Kuibyshevazot, Eurochem, and Acron, with units in the Southern Russian regions and Western Siberia, though the production units are located closer to the northwest of Kazakhstan. The source of carbon dioxide can be industrial production units which emit large quantities of this gas, so there are sources of carbon dioxide in large cities of Kazakhstan.

Regarding the economic side of the choice, in order to reduce both capital costs and operational expenses, it is more cost-effective to place the production unit on the territory of the special economic zone (SEZ). This type of area is dedicated to the placement of industrial facilities and gives privileges to residents. The important privileges are exemption and reduction of taxes, and availability of plug-and-play utilities such as water, electricity, and gas. There are 14 special economic

zones in Kazakhstan [59]. However, there are only four SEZs that specialize and have infrastructure for chemical production: National Industrial Petrochemical Technopark in Atyrau region, Pavlodar in Pavlodar city, Chemical Park Taraz in Taraz city, and Ontustik in Shymkent. The workforce availability is the same in all regions. A comparison of regions is shown in Table 5.1.

Considering the mentioned factors, the availability of feedstock from plants in Eastern Kazakhstan, availability of infrastructure and financial preferences make Atyrau the best choice for the location of the plant.

Factor	East Kazakhstan	West Kazakhstan	North Kazakhstan	South Kazakhstan	Central Kazakhstan
Raw materials	Ammonia production in Aktau, industrial plants including Kazazot, Atyrau refinery and KPI	Ammonia from Russian plants, industrial plants including Kazchrome, Kazzinc and Kazakhmys plants	Ammonia from Russian plants, few small production factories	Ammonium from Uzbekistan (small export of Uzbekistan), large distance from ammonia plants, few small production factories	Ammonium from Russian plants, no factories
Infrastructure and preferences	SEZ National Industrial Petrochemical Technopark	No special economic zones	SEZ Pavlodar	SEZ Chemical Park Taraz, SEZ Ontustik	No special economic zones
Market	Russia, Turkmenistan, nearest KZ market - North and South KZ	China, Russia, nearest markets - north and west of kazakhstan	Russia, nearest market - North Kazakhstan	Uzbekistan, nearest market - South Kazakhstan	Russia, nearest market - North and West Kazakhstan

Table 5.1: Comparison of KZ regions for plant construction

5.2 Plant layout

The total area of the plant is approximately 11 hectares. The exact location is shown, according to Google Earth service (Figure 5.1). Important considerations for the layout design include safety and process efficiency. The planned layout of the plant is shown in Figure 5.2.

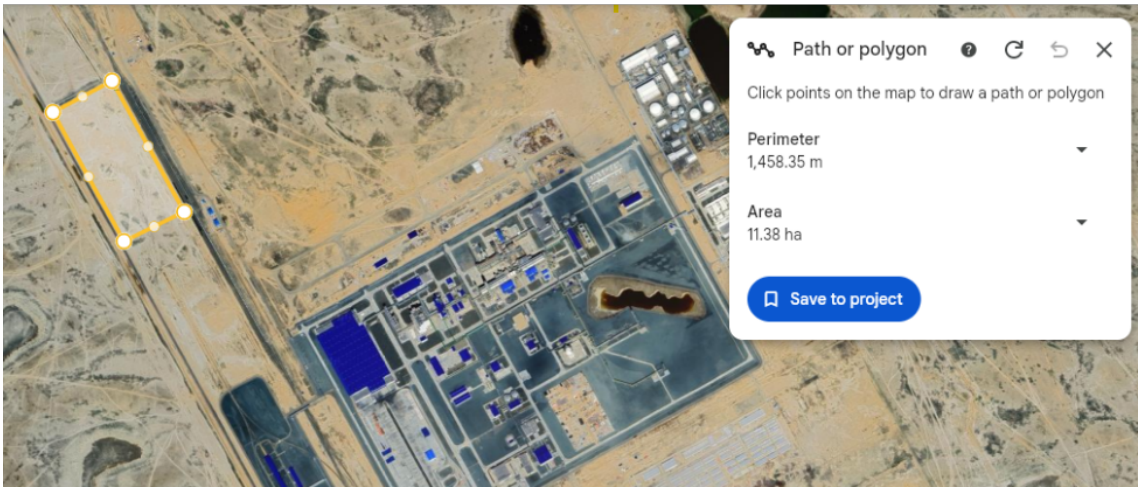

Figure 5.1: Plant location and area

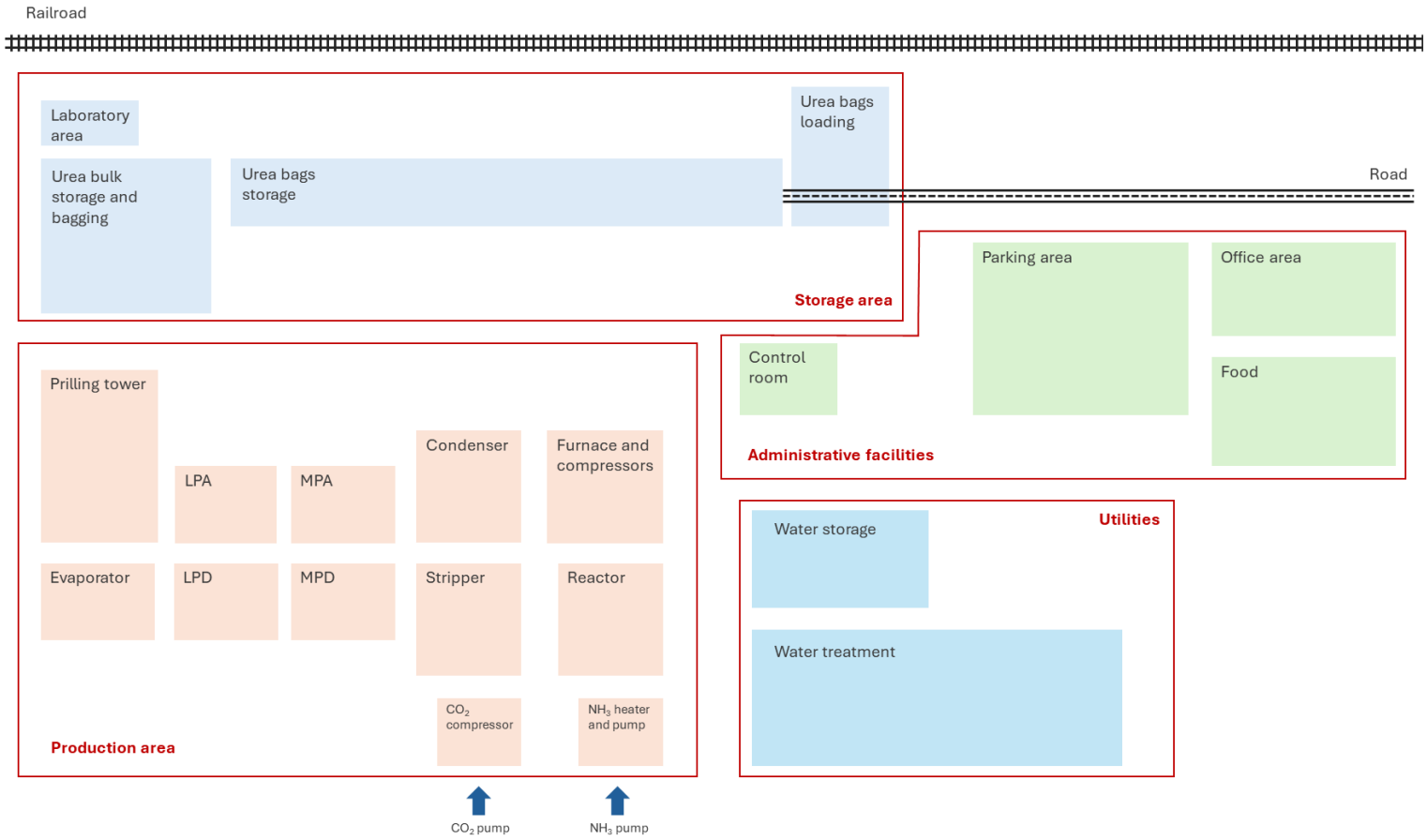

Figure 5.2: Plant layout

5.2.1 Production area

The chosen area is located furthest from the railroad and administrative buildings. It starts with the initial processing stages for the feedstock and ends with the prilling tower, from which urea is transported to the storage area. Besides major and minor production units, there is an additional area for heating in a furnace and compressors.

5.2.2 Storage area

The efficient packaging and transportation of the final product are essential for decreasing operating expenses and streamlining the production process. Urea granules from the stripper are transported into bulk storage, placed in big bags and then moved into bag storage. Due to proximity to the railroad and automotive roads, bags can be loaded with cargo crane lifts and machinery. Railroads that are needed for the planned transportation have already been constructed in the special economic zone. Also, the laboratory area allows for conducting experimental measurements of the final product.

5.2.3 Utilities

Water storage and water treatment sections are located near the production area and connected to a network of pipes. The water is sourced from the main pipeline of Astrakhan-Mangyshlak. Across the area of the plant, there are electrical networks that are connected to the national electrical grid.

5.2.4 Administrative facilities

The control room is a central administrative facility where operators and engineers monitor the process. It is located closer to the production site, although at a considerable distance for safety reasons. Other facilities include office areas for operators, engineers, laboratory technicians and other workers. There is also an area for a cafeteria.

Chapter 6

Environment and Waste streams

One of the main challenges faced by the urea manufacturing industry is waste management, particularly concerning the management of wastewater. The main source of this wastewater is the discharge stream from the evaporator unit (Stream 16) and prilling tower (Stream 19). From the evaporator, the water vapor (containing some impurities in the form of residual urea and biuret) is condensed and sent to the water treatment unit. From the prilling tower, the waste stream consists of residual urea. Despite the water being 99% pure, the remaining contaminants pose significant environmental hazards if discharged untreated. Hence, it is crucial to implement effective waste treatment techniques.

Component	**Mass flow ()**	**Mass fraction**
Water	7519.6	0.9983
Urea	12.8	0.0017

Table 6.1: Composition of Waste Stream from Evaporator

Component	**Mass flow ()**	**Mass fraction**
Air	73305.2	0.9985
Water	96.4	0.0013
Urea	12.8	174 ppm

Table 6.2: Composition of Waste Stream from Prilling Tower

According to the Ullmann's Encyclopedia of Industrial Chemistry [15], in the TOYO process, water condensate from evaporator with any residual contaminants

is sent to water treatment with hydrolysis, adsorption, and desorption (steam stripping), achieving effluent levels of contaminants (urea and ammonia) at 3–5 ppm in the wastewater before its removal from the urea plant [15]. The control of contaminant levels below 5 ppm aligns with global environmental regulations enforced by the EPA (Environmental Protection Agency) in the US and the EEA (European Environment Agency) in Europe.

Steps of water treatment

1. Hydrolysis

Hydrolysis is a chemical process where urea is broken down into simpler substances [15]. This is achieved by reacting urea with water and converting it back into carbon dioxide and ammonia. Hydrolysis is particularly effective in decomposing any residual urea in the wastewater, thus preventing it from entering the aquatic ecosystem where it could cause eutrophication [60].

2. Adsorption

In urea production, activated carbon, nano-iron phosphate, and fly ash adsorbents are used as adsorbents to remove dissolved contaminants like ammonia from the water [61]. During adsorption, these contaminants are trapped within the pore structure of the adsorbent material. This is a crucial step for removing lower molecular weight compounds that might not be fully addressed by hydrolysis alone [61]. Adsorption is effective in reducing concentrations of soluble impurities to very low levels, making it an essential part of ensuring that wastewater meets regulatory standards.

3. Desorption (Steam Stripping)

Desorption is used to remove any adsorbed ammonia and other volatile compounds from the treated water [60]. In steam stripping, steam is passed through the contaminated water, heating it and causing the volatile compounds to vaporize. These vapors are then captured and removed from the steam, which condenses back into a purified form [60]. This step is especially important for removing the last traces of ammonia, which is highly soluble in water and can be challenging to eliminate through other methods.

Effects on health

Urea can break down proteins, leading to skin irritation and damage by solubilizing the membrane of human skin. In the presence of saturated urea, the outer layer of the skin undergoes structural changes and loses its protective qualities, making it easier for microbes, allergens, and chemicals to penetrate. Saturated urea is also used in nail removal for its ability to dissolve nail structures [62]. Exposure to saturated urea solutions has been shown to reduce DNA synthesis and decrease epidermal thickness [62].

Effects on the environment

Ammonia and urea from urea production poses significant environmental and health risks. These releases can threaten air, water, and soil quality. Additionally, ammonia from urea contributes to acid rain, while nitrates in soil can leach into groundwater and the denitrification process releases nitrous oxide, further depleting the ozone layer [63].

Chapter 7

Total Investment and Profitability

7.1 General rules, equations and approximations

7.1.1 Cost Curve for Purchased Equipment Cost

The cost of the equipment parts is often calculated according to the Cost Curve for Purchased Equipment Cost, which assumes the material of construction to be stainless steel (Equation 7.1) [4].

$$C_e = a + bS^n \tag{7.1}$$

a, b - cost coefficient; S - size parameter, specific to equipment; n - exponent, specific to equipment.

7.1.2 Cost index

Cost indices for equipment cost approximations are widely used in industry to estimate relative cost over time. The cost index used in this report is the CEPCI factor, whose values are 509.7 for 2007 , 532.9 for 2010, and 825 for 2023 [64].

7.1.3 Location factor

To take into consideration the location factors, Russia is taken as a reference location, for which the location factor is 1.53. The closest Industrial Center in Russia is located in Chuvashia Republic. The location factor for Atyrau SEZ, where our plant will be located, is calculated by adding 10% for each 1000 miles of distance from Chuvashia

[4]. The distance between Atyrau and Chuvashia is 622 miles.

$$LF_{Atyrau} = 1.53 \times 1.1^{622/1000} = 1.62 \tag{7.2}$$

7.1.4 Material of Construction

The main material used for major units in the process is SAFUREX. Based on Table 7.1, it is clear that higher Chromium content leads to a higher factor, therefore, for SAFUREX, the same factor was taken as for 321 steel ($f_m = 1.5$), taking into account that for Hastelloy C, where the main component is Nickel, the factor is equal to 1.55.

Steel Grade	**304**	**316**	**321**	**SAFUREX**
Material Factor	1.3	1.3	1.2	1.5
Carbon (%)	0.08	0.08	0.08	0.03
Chromium (%)	18-20	16-18	17-19	29
Nickel (%)	8.0-10.5	10-14	9-12	6.5

Table 7.1: Comparison of steel grades [11]

7.2 Cost of Reactor

The reactor has the following components: storage tank with volume of 300 m^3 and 10 sieve trays with diameters of 4.2 m. The material of construction is SAFUREX. The purchased cost of the storage tank is calculated using the Cost Curve for Purchased Equipment (Equation 7.1) with the corresponding parameters [4].

$$C_{storagetank} = 113,000 + 3250 \times 300^{0.65} = \$246,000$$

The purchased cost of 10 sieve trays are:

$$C_{tank} = 10 \times (130 + 400 \times 3.9^{1.8}) = \$48,000$$

The installed cost of the reactor is estimated as follows (for detailed calculations, see Appendix G):

$$C_{installed} = \$1,200,000$$

The estimated cost is the cost on a U.S. Gulf Coast basis in 2010. Calibrating the cost to a Kazakhstan basis in 2024 to obtain the Inside Battery Limit Cost (ISBL):

$$C_{reactor} = \$3,000,000$$

7.3 Cost of Stripper

The surface area of the stripping unit is 76.55 m^2. The cost of the stripping unit was calculated based on the Cost Curve Method for Purchased Equipment (see Section 7.1). The material of the unit is SAFUREX stainless steel alloy. Purchased Equipment cost for the U-tube shell and tube heat exchanger was used, with the falling film type heat exchanger more closely resembling the stripper in this process.

$$C = 28,000 + 54 \times 76.55^{1.2} = \$38,000 \tag{7.3}$$

The installation factor of 3.5 for heat exchangers from Hand (1958) was used [4]. Multiplication by the installation factor and material factor resulted in a total cost of $200,000. Moreover, the cost was adjusted to inflation (CEPCI index) and the total cost adjusted for inflation factor is $310,000. Considering the location factor, the cost is equal to $500,000.

7.4 Cost of Condenser

A carbamate condenser is a U-tube shell and tube heat exchanger with a surface area of 534.4 m2. The cost was calculated based on the Cost Curve Method for Purchased Equipment using Equation 7.1. The material of the unit is SAFUREX stainless steel alloy.

$$C = 24,000 + 46 \times 534.4^{1.2} = \$110,000 \tag{7.4}$$

The estimated cost is the cost on a U.S. Gulf Coast basis in 2007 (CEPCI = 509.7). Calibrating the cost to a Kazakhstan basis in 2024 gives:

$$C = 110,000 \times \frac{825}{509.7} = \$180,000 \tag{7.5}$$

Multiplication by installation factor for heat exchanger proposed by Hand (3.5) and material factor (1.5) results in a cost of $940,000.
Considering the location factor(1.62), the Inside Battery Limit Cost (ISBL):

$$C_{condenser} = \$1,500,000$$

7.5 Cost of Evaporator

According to Woods (2007) [65] as a rule of thumb in engineering practice, the cost of the equipment is given by:

$$C_e = C_{base} \times (\frac{Actual\ area}{Base\ area})^n \times (L + M^*) \tag{7.6}$$

Woods (2007) [65] reports that the cost of the falling film evaporator, equipped with a vacuum drum, steam piping, long tubes, and barometric condenser is set at $350,000 FOB (Free On Board) for a heat transfer area of 100 m². The cost scaling exponent n is 0.68. The Lang factor ($L + M^*$, Labor + materials) for estimating the total installed cost is 2.5, and the labor to materials cost ratio (L/M) is 0.35. The base FOB cost is $350,000 for the CEPCI 1000[65], and the CEPCI in 2023 is 825. Adjusted FOB Cost is:

$$FOB_{Adjusted} = \$350,000(825/1000) = \$288,750$$

The FOB cost adjusted for the year 2023, with a CEPCI of 825, would be approximately $288,750. This reflects the economic conditions and changes in the cost of materials and labor relative to the base year. The evaporator material is set to Carbon Steel which has a multiplier of 1.00 (standard material, no additional cost). As a result, the cost of the evaporator is:

$$C_e = \$288,750 \times \frac{106}{100}^{0.68} 2.5 \approx \$750,000 \tag{7.7}$$

The cost of the falling film evaporator, equipped with a vacuum drum, steam piping, long tubes, and barometric condenser is calculated to be $750,000 including installation and materials costs.

7.6 Cost of Prilling Tower

The prilling tower consists of a long tower (74 m in height), a spray to form urea droplets for further crystallization and droplet distribution over the diameter of the prilling tower, a pump for inlet urea melt, a sump for residual liquid at the bottom of the tower, a scrubber to avoid and lessen the undesirable urea dust [66], and ductwork to provide countercurrent air flow. Excluding the devices for control of air pollution, the above-mentioned prilling tower constituents are reported to compose a prilling tower equipment cost of 14,250,000 dollars in 2007, with n = 0.57, range equal to 300-1200 and prilled capacity of 1000 tonnes/d [65].

$$C_2 = C_{ref} \times (\frac{Size_2}{Size_{ref}})^n \tag{7.8}$$

The subscript 2 refers to predicted equipment, ref refers to reference equipment. size - flow or capacity of the equipment, tonnes per day for the prilling tower. Based on the Equation 7.8, the cost of the prilling tower in the process is estimated to be $11,000,000. The cost is updated to $17,000,000 based on the CEPCI index as the initial cost is reported for the year 2007.

7.7 Total Plant Cost

All the calculations for the equipment costs resulted in Inside Battery Limits (ISBL) costs, which account for the costs associated with expenses inside the physical boundaries of the equipment construction, such as piping. For the total cost, Outside Battery Limits cost should also be estimated. OSBL accounts for costs associated with expenses outside the physical boundaries, such as land acquisition, logistics and utilities. OSBL cost is conventionally approximated as 40% of the ISBL cost. The equipment costs and the total cost of the plant are summarized in Table 7.2. The total cost of the plant is estimated to be $32,000,000.

7.8 Economic Analysis

7.8.1 Revenue

The price of selling urea was assumed as the average price for the previous year, which is $370 per tonne [67]. Since it is expected that 225,000 tonnes of urea will

Equipment	ISBL Cost ($)	Total Cost ($)
Reactor	3,000,000	4,200,000
Stripper	500,000	700,000
Condenser	1,500,000	2,100,000
Evaporator	750,000	1,000,000
Prilling tower	17,000,000	23,800,000
Total		**32,000,000**

Table 7.2: Summary of Separate Costs on Major Equipment for Urea Production

be sold annually, the total revenue for Year 1 is $66 mln. For the following period, revenue, as well as operating expenses, are indexed according to the average U.S. inflation rate (2.51%).

7.8.2 Expenses

Cost of reagents

Urea plants are profitable due to the integration of ammonia and urea production (or other ammonia fertilizers). For our plant, it was assumed that the price of ammonia is $95 per tonne, which is the prime cost of ammonia production for the KazAzot plant [12]. The purchase of ammonia at the market price for a urea plant is economically non-feasible. The price of CO_2 was assumed to be equal to EU carbon permits ($68 per tonne) [68].

	2020	2021	2022
Prime ammonia cost, KZT/year	760,117,000	836,152,000	858,640,000
Ammonia sold, tonnes	23,960	22,860	19,570
Price, KZT/tonne	31,724	36,577	43,875
Price, $/tonne	68.97	79.52	95.38

Table 7.3: Prime Ammonia cost for KazAzot [12]

Cost of labor

Two types of jobs at the production site that were accounted for are operators and supervisors. While operators are responsible for monitoring plant operations and minor troubleshooting, supervisors are more qualified process engineers responsible for overseeing plant operations and managing personnel. Also, supervisors include safety engineers, quality control engineers and instrumentation and control engineers.

According to Seider et al. [69], for a continuous operation 1 operator is required per process section for the process step that includes fluids processing and 2 operators for solids-fluids processing. It is also assumed that for every 5 operators, there will be a single supervisor. In total, the number of workplaces is 12 (see Electronic Supplementary Information). Each shift of a worker is 8 hours. The number of shifts per workplace:

$$N_s = 3\ shifts/day \times 365\ days = 1095\ shifts/year/workplace \tag{7.9}$$

It is assumed that a single worker is able to work 5 shifts a week, 48 weeks a year (excluding a minimum vacation period of 24 days or about 4 weeks). The number of shifts per worker:

$$N_{s/w} = 5\ shifts/week \times 48\ weeks/year = 240\ shifts/year/worker \tag{7.10}$$

So, the number of workers per workplace:

$$N_{w/p} = \frac{1095\ shifts/year/workplace}{240\ shifts/year/worker} \approx 5\ worker/workplace \tag{7.11}$$

Therefore, the total number of workers required is 60 people (50 operators and 10 supervisors). According to the National Bureau of Statistics of Kazakhstan, the average monthly salary of a chemical engineer in the oil and gas industry in 2023 is 790,490 KZT, of an operator at an oil processing unit is 402,100 KZT, and of a laboratory chemist is 238,000. With 40 hours worked per week, the hourly rate is equal to $10.7 for an engineer, $5.5 for an operator, and $3.2 for a laboratory chemist. This already includes all taxes and other payments for a worker, according to the methodology of the bureau [70]. For the control laboratory, 1 workplace should be filled (in total, 5 workers). According to Seider [69], apart from direct wages, salaries and benefits should be accounted for, which is 15% of direct wages.

Also, operating supplies and services are equal to 6% direct wages. In total, wages, salaries, benefits and operating supplies and services are $900,000.

Maintenance cost

Maintenance wage and benefits are 4.5% of the total depreciable capital, $1,575,000. Moreover, salaries and benefits are 25% of maintenance wage and benefits, material and services for maintenance are 100% of the same value, and maintenance overhead is 5%. In total, maintenance expenses are $2,047,500.

Overhead

Overhead expenses are calculated as 22,8% of labor and maintenance cost, which is equal to $670,000.

Taxes

Corporate income tax is equal to 20% of the taxable income (EBIT).

Depreciation

The linear depreciation model was applied for 20 years, with an annual depreciation value of $1,600,000.

Rent

According to QazIndustry, investors in the special economic zone are freed from rent payments [71].

Operating expenses (Utilities)

According to Seider [69], the cost of utilities is 5-10% of the selling price of the product. Since the process requires high pressures and temperatures at major units (but not higher than 200 °C), the cost of utilities was assumed to be 9% of the revenue.

Net Working Capital

Net working capital is the difference between the sum of cash, accounts receivable and inventories and the sum of accounts payable and debts. Since the customers are in different regions and countries, account receivables are high. This also increases the inventory, which is also affected by the seasonality of the final product. Therefore, it was assumed that the net working capital is 80% of gross profit.

Other assumptions

The cost of capital was assumed to be 15%. Assuming that the company's capital structure will primarily consist of debt, the decrease in the estimated cost of capital is reasonable.
The exchange rate of KZT to U.S. dollar 460 KZT / 1 $.
Projections were made for 20 years from 2025.
The growth rate (3%) is assumed to be slightly higher than the inflation rate.

Profitability

Figure 7.1 illustrates the changes in cumulative cash flow generated by the plant, taking into account the capital cost of the plant, and further projections of its net income for the next 20 years. The payback period of the plant was calculated based on the amount of cumulative cash flow. The cumulative cash flow is $-1.996 mln in year 5 and $8.659 mln in year 6 (see ESI). The payback is equal to the date at which cumulative cash flow will be zero.

$$Payback\ period = 5 + \frac{0 - (-1.996)}{8.659 - (-1.996)} = 5.2 years. \tag{7.12}$$

Considering the large amount of investments, the plant has a relatively low payback period. The net present value (NPV) of the plant was calculated as the sum of the discounted cash flows through 20 years and the terminal value. At the cost of capital (discount rate) of 15%, the net present value was equal to $26.6 mln. Figure 7.2 demonstrates the change of NPV as the cost of capital increases. Moreover, the ROI was found to be 26%, and the pre-tax ROI was estimated as 33%. Sensitivity analysis of the feedstock price, shown in Figure 7.3 demonstrates a high dependence of NPV on the prices of NH_3 and CO_2. The minimum price of NH_3 for the plant to have a positive NPV is about $130 per tonne, and for CO_2 such price is $40 per tonne.

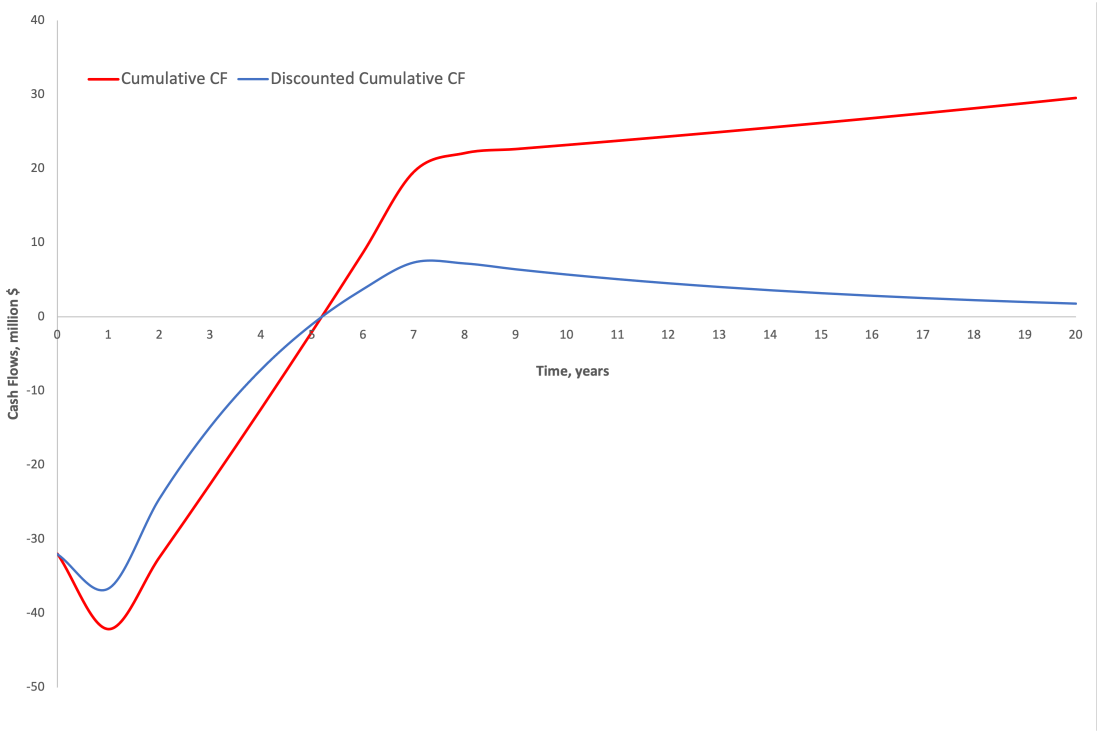

Figure 7.1: Cumulative cash flow of the Urea Production Plant

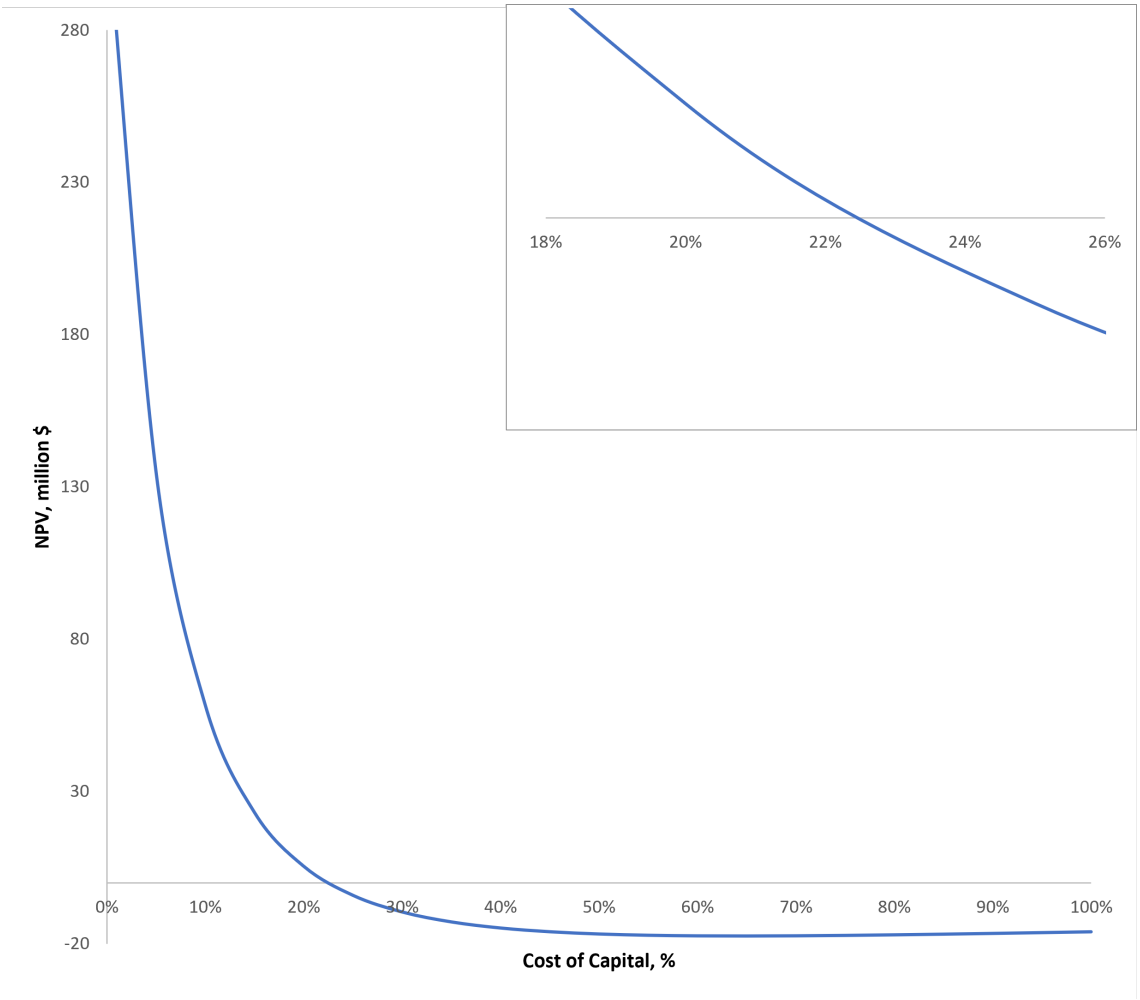

Figure 7.2: Sensitive analysis of NPV against the cost of capital

	NH3 price										
	50	60	70	80	90	100	110	120	130	140	150
CO2 price											
40	144	125	107	88	70	52	35	18	1	-16	-33
50	128	109	90	72	55	37	20	3	-14	-31	-47
60	111	93	75	57	40	22	5	-12	-28	-45	-61
70	96	77	59	42	25	8	-9	-26	-42	-58	-74
80	80	62	44	27	10	-7	-24	-40	-56	-72	-88
90	64	47	29	12	-5	-21	-38	-54	-70	-86	-101
100	49	32	14	-3	-19	-36	-52	-68	-83	-99	-114
110	34	17	0	-17	-33	-50	-66	-81	-97	-112	-127
120	19	2	-15	-31	-47	-63	-79	-95	-110	-125	-140
130	4	-12	-29	-45	-61	-77	-93	-108	-123	-138	-152
140	-10	-27	-43	-59	-75	-90	-106	-121	-136	-150	-165
150	-24	-41	-57	-73	-88	-104	-119	-134	-148	-163	-177

Figure 7.3: Sensitive analysis of NPV against feedstock price

Chapter 8

Conclusions and Future Work

To sum up, a thorough report on Design of Urea Production Plant in Kazakhstan is presented. The report includes identification of the key characteristics of the plant, such as the plant capacity and the process technology, creation of material balance and the Process Flow Diagram for the plant operation, detailed and rigorous design of the major units and comprehensive description of the minor units of the process, considerate suggestions for the location and layout of the plant, plans for the treatment of waste streams and its environmental considerations, cost estimations for the purchase of major units and total plant construction, and complete economic analysis for the whole period of plant operation.

The information and calculations provided in the report are invaluable for the process of urea production and are often rigorous and hard-sought, which adds to the value of the document. The designs and suggestions of the report can be readily and reliably used for the construction of a urea plant in Kazakhstan and will be a good source of insights and ideas, as well as a dependable reference.

For further improvement of the equipment design and process simulations of the urea production plant, detailed modelling of the urea synthesis reaction, including the states of its components, requirements, thorough and versatile kinetics, and a comprehensive description of the stages of the reaction should be devised. For the moment, such a model doesn't seem to exist, which, perhaps, inhibits the design and efficiency of the urea production processes.

Bibliography

[1] Paul Dean. How to read a risk matrix used in a risk analysis, Feb 2024.

[2] Mohsen Hamidipour, Navid Mostoufi, and Rahmat Sotudeh-Gharebagh. Modeling the synthesis section of an industrial urea plant. *Chemical Engineering Journal*, 106(3):249–260, 2005.

[3] Towler Gavin Sinnott, Ray K. 12.10.3 condensation inside and outside vertical tubes, 2009.

[4] Gavin Towler and Ray Sinnott. *Chemical engineering design: principles, practice and economics of plant and process design*. Butterworth-Heinemann, 2021.

[5] TOYO Engineering. Aces21 urea process by toyo. https://www.toyo-eng.com/jp/en/solution/energy/pdf/ACES21_Brochure.pdf, n.d. Accessed: April 20, 2024.

[6] Shijun Guo, Shubham Sharma, Alibek Issakhov, and Nima Khalilpoor. Evaluation of the safety of high-salt wastewater treatment in coal chemical industry based on the ahp fuzzy method. *Journal of Chemistry*, 2021:1–7, 2021.

[7] Il Seouk Park and Man Young Kim. Numerical investigation of the heat and mass transfer in a vertical tube evaporator with the three-zone analysis. *International journal of heat and mass transfer*, 52(11-12):2599–2606, 2009.

[8] Dresser-rand hoss compressor. https://p3.aprimocdn.net/siemensenergy/c76084f5-b4ab-4088-879b-b05000a7b9b8/HOSS-Specification-Sheet-June-2021-pdf_Original%20file.pdf. Accessed: 2024-03-13.

[9] Ray Sinnott and Gavin Towler. *Chemical engineering design: SI Edition*. Elsevier, 2009.

[10] R. Turton. *Analysis, Synthesis, and Design of Chemical Processes*. Prentice-Hall international series in engineering. Prentice Hall, 2012.

[11] Rolled Metal Products. Stainless steel type 321. https://rolledmetalproducts.com/stainless-steel-type-321/, n.d. Accessed: April 15, 2024.

[12] KazAzot. Kazazot annual report. https://kase.kz/files/emitters/KZAZ/kzazp_2022_rus.pdf, December 2022.

[13] Jozef Meessen. Urea synthesis. *Chemie Ingenieur Technik*, 86(12):2180–2189, 2014.

[14] C Kurt and J Bittner. Sodium hydroxide. ullmann's encyclopedia of industrial chemistry, 2003.

[15] Jozef H Meessen. Urea. *Ullmann's Encyclopedia of Industrial Chemistry*, 2010.

[16] Justin G Driver, Rhodri E Owen, Terence Makanyire, Janice A Lake, James McGregor, and Peter Styring. Blue urea: fertilizer with reduced environmental impact. *Frontiers in Energy Research*, 7:88, 2019.

[17] Toyo Engineering Inc. Energy-saving urea synthesis technology: Aces21. https://www.toyo-eng.com/jp/en/solution/energy/.

[18] Rommel Ortiz Guzmán and Antonio Bueno Lazo. Simulation of a reactor considering the stamicarbon, snamprogetti, and toyo patents for obtaining urea. *Open Chemistry*, 20(1):424–430, 2022.

[19] Dale E Seborg, Thomas F Edgar, Duncan A Mellichamp, and Francis J Doyle III. *Process dynamics and control*. John Wiley & Sons, 2016.

[20] Guidelines for investigating chemical process incidents. https://www.aiche.org/resources/publications/books/guidelines-investigating-chemical-process-incidents-2nd-edition. Accessed: 2024-03-14.

[21] Uddipta Mondal, Nishat Salsabil, and Easir A Khan. Safety performance assesment of hazardous chemical facilities in bangladesh using indexing approach. *Chemical Engineering Research Bulletin*, 22, 2020.

[22] Prem Baboo and Mark Brouwer. How to improve safety and reliability of the high pressure synthesis section of urea plants. 03 2021.

[23] Luc Vandebroek, Filip Verplaetsen, Jan Berghmans, A Van den Aarssen, H Winter, G Vliegen, and E Van't Oost. Auto-ignition hazard of mixtures of ammonia, hydrogen, methane and air in a urea plant. *Journal of hazardous materials*, 93(1):123–136, 2002.

[24] Prem Baboo, Mark Brouwer, Jo Eijkenboom, and Majid Mohammadian. The lessons learned from the first 100 safety hazards in urea plants the lessons learned from the first 100 safety hazards in urea plants. 09 2018.

[25] XP Zhang, PJ Yao, Dan Wu, and Yi Yuan. Simulation of urea reactor of industrial process. *WIT Transactions on Engineering Sciences*, 30, 2001.

[26] Mario Dente, Sauro Pierucci, Angelo Sogaro, G Carloni, and E Rigolli. Simulation program for urea plants. *Computers & chemical engineering*, 12(5):389–400, 1988.

[27] H Scott Fogler. *Elements of chemical reaction engineering*. Pearson, 2020.

[28] Maria Zolotajkin, Jozef Szarawara, and Jerzy Piotrowski. Kinetic equation of the urea-synthesis process. https://ureaknowhow.com/wp-content/uploads/2014/11/1984-Zolotajkin-Kinetic-equation-of-the-urea-synthesis-process.pdf, 1984.

[29] Yara International ASA. Cn113710341b - high-pressure stripper for use in a urea plant. https://patents.google.com/patent/CN113710341B/en. Accessed: 2024-03-15.

[30] S. Schbib D. Cesari and D. Borio. Steady state analysis of a falling film reactor. *2nd Mercosur Congress on Chemical Engineering*, 2005.

[31] Stamicarbon BV. Cn113993603b - urea plant with stripper and stripping method. https://patents.google.com/patent/CN113993603B/en. Accessed: 2024-03-15.

[32] N. Mustoufi M. Hamidipour and R. Sotudeh-Gharebagh. Modelling the synthesis section ofan industrial ureaplant. *Chemical Engineering Journal*, 106:249–260, 2005.

[33] Prem Baboo. Some fact about urea stripper. 2022.

[34] THERMOPERDIA. https://www.thermopedia.com/content/1150/, Jun 2011.

[35] Maria D Cardona, Gerardo Alcala, Cesar A Ramirez, Dario Colorado, and Fernando Rueda. New methodology for the determination of the failure times in an ammonium carbamate condenser. *Chemical Engineering Transactions*, 70:1813–1818, 2018.

[36] Stamicarbon. Carbamate condenser. https://www.stamicarbon.com/advance-design-safurex-high-pressure-carbamate-condenser, n.d. Accessed: April 20, 2024.

[37] Renata Chinda, Carlos Yamamoto, Daniel Lima, and Fernando Pessoa. Industrial urea process–simulation and validation. *Int j Adv Eng Res Sci*, 6:324, 2019.

[38] YA Sergeev, RV Anderzhanov, and AA Vorob'Ev. Energy-and resourse-saving technologies and equipment in urea production. *Russian Journal of General Chemistry*, 90:1168–1172, 2020.

[39] Archie Vivian Slack. Urea technology: A critical review. 1969.

[40] Jing Fang, Kaixuan Li, and Mengyu Diao. Establishment of the falling film evaporation model and correlation of the overall heat transfer coefficient. *Royal Society Open Science*, 6(5):190135, 2019.

[41] Ali Mehrez, Ahmed Hamza H Ali, WK Zahra, S Ookawara, and M Suzuki. Study on heat and mass transfer during urea prilling process. *International Journal of Chemical Engineering and Applications*, 3(5):347, 2012.

[42] WU Yuan, BAO Chuanping, and ZHOU Yuxin. An innovated tower-fluidized bed prilling process. *Chinese Journal of Chemical Engineering*, 15(3):424–428, 2007.

[43] I Mavrovic. Process for prilling urea. https://patents.google.com/patent/US3836611A/en. Accessed: 2024-03-14.

[44] Urea. https://www.palamaticprocess.com/powder-urea. Accessed: 2024-03-14.

[45] Sauli Halonen, Teija Kangas, Mauri Haataja, and Ulla Lassi. Urea-water-solution properties: Density, viscosity, and surface tension in an undersaturated solution. *Emission Control Science and Technology*, 3:161–170, 2017.

[46] Bastian Rapp. *Microfluidics: Modeling, Mechanics and Mathematics*. Elsevier, 2017.

[47] Saad N Saleh, Shakir M Ahmed, Dawood Al-mosuli, and Shahzad Barghi. Basic design methodology for a prilling tower. *The Canadian Journal of Chemical Engineering*, 93(8):1403–1409, 2015.

[48] Maksym Skydanenko, Vsevolod Sklabinskyi, Saad Saleh, and Shahzad Barghi. Reduction of dust emission by monodisperse system technology for ammonium nitrate manufacturing. *Processes*, 5(3):37, 2017.

[49] N Rahmanian, M Homayoonfard, and A Alamdari. Simulation of urea prilling process: An industrial case study. *Chemical Engineering Communications*, 200(6):764–782, 2013.

[50] Carl L. Yaws. *Yaws' Critical Property Data for Chemical Engineers and Chemists*. Knovel, 2012; 2013; 2014.

[51] Editor Engineeringtoolbox. Air - specific heat vs. temperature at constant pressure. *Engineering ToolBox*, Feb 2024.

[52] J. D Rodríguez García, Miguel Asuaje, Eduardo Pereyra, and Nicolás Ratkovich. Analysis of two-phase gas-liquid flow in an Electric Submersible Pump using A CFD approach. *Geoenergy Science and Engineering*, 233:212510, 2 2024.

[53] Christin Barney. Heat exchange system for reforming in an ammonia process.

[54] Waheed Ahmad, Mirpur Mathelo, and Fauji Fertilizer Company. Revamp of the Medium Pressure Decomposer at Fauji Fertilizer Company Ltd Mirpur Mathelo (former Pak Saudi Fertilizer), 8 2011.

[55] Urea storage, calibration and application – follow our best practice guide.

[56] Pestell Minerals Ingredients. Urea - Prills — Pestell Nutrition, 7 2021.

[57] Merit chemicals (n.d.). https://meritchemicals.com/en/product-detail/1111111111karbamid.

[58] A. Kelebayeva. KIOGE - AO "KazAzot" - yedinstvennyy proizvoditel' ammiaka i ammiachnoy selitry v RK. https://shorturl.at/GRY38, n.d. Accessed on: April 20, 2024.

[59] Invest In Kazakhstan — Special Economic Zones. https://invest.gov.kz/doing-business-here/fez-and/the-list-of-sez-and/, n.d. Accessed on: April 20, 2024.

[60] L. Matijašević, I. Dejanović, and H. Lisac. Treatment of wastewater generated by urea production. *Resources, Conservation and Recycling*, 54(3):149–154, 2009.

[61] A. Zaher and N. Shehata. Recent advances and challenges in management of urea wastewater: A mini review. *IOP Conference Series: Materials Science and Engineering*, 1046(1):012021, 2021.

[62] Marie Lodén. Clinical evidence for the use of urea. In *Dry Skin and Moisturizers*, pages 227–242. 2005.

[63] Agung S. Danasa, Teguh E. Soesilo, Dwi N. Martono, Agus Sodri, Akhmad S. Hadi, and Guntur T. Chandrasa. The ammonia release hazard and risk assessment: A case study of the urea fertilizer industry in indonesia. *IOP Conference Series: Earth and Environmental Science*, 399(1):012087, 2019.

[64] Economic indicators. *Chemical Engineering*, 130(6):825, June 2023.

[65] Donald R. Woods. *Appendix D: Capital cost guidelines*, pages 376–436. 2007.

[66] E. Sakata and T. Yanagawa. *Latest Urea Technology for Improving Performance and Product Quality*. Technology & Knowledge Research Centre, Tokyo Engineering Corporation, Japan, 2002.

[67] Trading Economics. Urea. https://tradingeconomics.com/commodity/urea. Accessed: 21 April 2024.

[68] Trading Economics. Carbon dioxide. https://tradingeconomics.com/commodity/carbon. Accessed: 21 April 2024.

[69] Warren D Seider, Junior D Seader, and Daniel R Lewin. Process design principles: synthesis, analysis, and evaluation. *(No Title)*, 1999.

[70] National Bureau of Statistics. Salaries and working conditions. https://stat.gov.kz/ru/methodology/28585/. Accessed: 21 April 2024.

[71] QazIndustry. Special economic industrial zones in kazakhstan. https://qazindustry.gov.kz/docs/sez/sez-iz-rk.pdf. Accessed: 21 April 2024.

[72] Hassan Hafiz, Salim Muhammad, Rasool Noman, and Usman Muhammad. Toyo's aces process for urea synthesis, 2014.

[73] Chao Luo, Jun Zhao, and Weibin Ma. Heat-transfer characteristics of ammonia-water falling film generation outside a vertical tube. *Thermal Science*, 21(3):1251–1259, 2017.

[74] IIAR. Chapter 2 — properties of ammonia. thermodynamic properties of ammonia. May 2008.

[75] LT Carmichael, HH Reamer, and Bruce Hornbrook Sage. Viscosity of ammonia at high pressures. *Journal of Chemical and Engineering Data*, 8(3):400–404, 1963.

[76] Weidenfeller. High performance steam super-heater in ammonia production lines. 2017.

[77] SKI. Properties of water and steam. https://www.ski-gmbh.com/swa/tools/steam. Accessed: 2024-03-15.

[78] engineeringtoolbox. Water - thermal conductivity vs. temperature. https://www.engineeringtoolbox.com/water-liquid-gas-thermal-conductivity-temperature-pressure-d_2012.html. Accessed: 2024-03-15.

Appendix A

Reactor Design calculations

A.1 Mass transfer

The mass transfer between the liquid and gaseous phases in the reactor can be modeled using the two-film theory model. Mass transfer flux of a component through vapor and liquid films are [25]:

$$N_i^G = k_i^G \cdot \left(y_i - y_i^I\right) \tag{A.1}$$

$$N_i^L = k_i^L \cdot \left(x_i^I - x_i\right) \tag{A.2}$$

Equilibrium of the component in the phase interface is represented as:

$$y_i^I = m_i \cdot x^I \tag{A.3}$$

Material balance at the phase interface:

$$N_i^G = N_i^L \tag{A.4}$$

Combining the equations to eliminate the interfacial component mole fractions:

$$N_i^G = K_i^G \cdot (y_i - m_i x_i) \tag{A.5}$$

Where,

$$\frac{1}{K_i^G} = \frac{1}{k_i^G} + \frac{m_i}{k_i^L} \tag{A.6}$$

A.2 Heat transfer

The calculations for the heat of Ammonium Carbamate formation are shown below.

$$\Delta H_r(T) = \Delta H_r^{\circ} + \int_{T_1}^{T} C_p(T)\, dT \tag{A.7}$$

$$\begin{aligned} \Delta H_r = &-117.0\frac{kJ}{mol} + 2.590\frac{kJ}{kg.K} \times 78.10\frac{g}{mol} \times \\ &\times \frac{1kg}{1000g} \times (463K - 300K) = -84.03\frac{kJ}{mol} \end{aligned} \tag{A.8}$$

$$\begin{aligned} \dot{Q_1} &= \Delta H_r \times \dot{F_{CO2}} \times X_1 \\ &= -84.03\frac{kJ}{mol} \times 164.3\frac{kmol}{h} \times \frac{1000mol}{1kmol} \times \frac{1h}{3600s} \\ &= -3835kW \end{aligned} \tag{A.9}$$

The enthalpy change of Ammonium Carbamate's decomposition to urea and water is calculated according to Equation A.7:

$$\Delta H_r = \Delta H_r^{\circ} + \int_{T_1}^{T} (C_{p(water)}\, dT \tag{A.10}$$

$$\begin{aligned} \Delta H_r = &+15.50\frac{kJ}{mol} + \int_{300}^{463} (2.764e5 - 2090T + 8.125T^2 \\ &- 0.01412T^3 + 9.370e-6T^4)\, dT \\ &= 15.50\frac{kJ}{mol} + 12.46\frac{kJ}{mol} = 27.96\frac{kJ}{mol} \end{aligned} \tag{A.11}$$

$$\begin{aligned} \dot{Q_2} &= \Delta H_r \times (\dot{F_{CO2}} + \dot{F_{NH4CO2NH2}}) \times X \\ &= 27.96\frac{kJ}{mol} \times (164.3 + 515.2)\frac{kmol}{h} \times \frac{1000mol}{1kmol} \times \frac{1h}{3600s} \times 0.63 \\ &= 3282kW \end{aligned} \tag{A.12}$$

The net energy of the reactor:

$$\dot{Q}_{\text{reactor}} = \dot{Q_1} + \dot{Q_2} \tag{A.13}$$

$$\dot{Q_{\text{reactor}}} = -3835kW + 3282kW = -553kW \tag{A.14}$$

A.3 Reactor Sizing

$$V = 679.5\text{kmol/m}^3 \times$$
$$\times \int_0^{0.63} \frac{dX}{0.053 \cdot (C_{A0} \cdot (1-X))^{0.7} - 0.046 \cdot (C_{A0} \cdot X)} \cdot (C_{W0} + C_{A0} \cdot X)^{-0.4} \quad \text{(A.15)}$$

$$C_{A0} = \frac{F_{A0}}{Q_0} \quad \text{(A.16)}$$

The integral in Equation A.15 was solved numerically using Python Scipy Library, and the volume was determined.

A.4 Nomenclature

N_i^G, N_i^L - mass transfer of component i through gas and liquid films
k_i^G, k_i^L - mass transfer coefficients through gas and liquid film
K_i^G - overall mass transfer coefficient
$y_i x_i$ - bulk molar concentrations
y_i^I, x_i^I - interfacial molar concentrations
m_i - pseudo-equilibrium constant

Appendix B

Stripper Design Calculations

B.1 Heat duty

The energy consumption for heating is calculated as the sum of energies to heat urea, water, a part of ammonia and unreacted ammonia carbamate that goes to the medium pressure decomposer. Equation B.1 demonstrates energy consumption for heating urea:

$$\dot{Q}_1 = 427.7\frac{kmol}{hr} \times 94\frac{J}{mol \times K} \times 5K = 0.056MW \tag{B.1}$$

For water:

$$\dot{Q}_2 = 428.1\frac{kmol}{hr} \times 80.2\frac{kJ}{kmol \times K} \times 5K = 0.048MW \tag{B.2}$$

For ammonia:

$$\dot{Q}_3 = 426.9\frac{kmol}{hr} \times 35\frac{J}{mol \times K} \times 5K = 0.021MW \tag{B.3}$$

For ammonium carbamate:

$$\dot{Q}_3 = 211.2\frac{kmol}{hr} \times 2.59\frac{kJ}{kg \times K} \times 78.07\frac{kg}{kmol} \times 5K = 0.06MW \tag{B.4}$$

Decomposition energy of Ammonium Carbamate to CO2 and NH3 requires the amount of energy calculated by equation B.6:

$$\Delta\dot{H} = 117\frac{kJ}{mol} \tag{B.5}$$

$$\dot{Q}_4 = 117\frac{kJ}{mol} \times 40.2\frac{kmol}{h} \times 1000\frac{mol}{1kmol} \times \frac{1hr}{3600s} = 1.3065MW \tag{B.6}$$

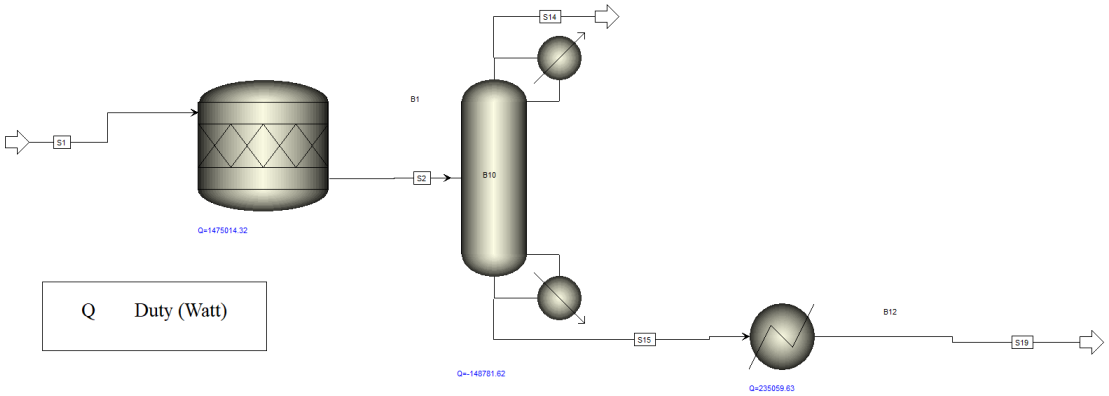

Figure B.1: Aspen Plus V14 simulation of stripping column

Total heat required for a stripper is

$$\dot{Q} = \dot{Q}_1 + \dot{Q}_2 + \dot{Q}_3 + \dot{Q}_4 = 1.49MW \tag{B.7}$$

Aspen Validation

The energy requirement of the stripping column was validated in Aspen Plus program, as shown in Figure B.1. In order to recreate the process, reaction of ammonium carbamate decomposition was conducted in RStoic reactor, and then, the mixture was separated into carbon dioxide and part of ammonia in the gas phase and other components in the liquid phase. The net heat duty of all units was found to be equal to 1.511KW, which is close to the one calculated manually.

Appendix C

Condenser Design Calculations

C.1 Heat duty

Estimated CO_2 conversion in condenser is 0.65. As ΔH_r for Ammonium Carbamate was calculated before, the heat of Ammonium Carbamate formation is shown below.

$$\Delta H_r = -84.03 \frac{kJ}{mol}$$

$$\dot{Q_1} = \Delta H_r \times \dot{F_{CO2}} \times X_1 = -84.03 \frac{kJ}{mol} \times 469.5 \frac{kmol}{h} \times \frac{1h}{3600s} \times 0.65 = -7.123\text{MW} \tag{C.1}$$

The heat released from unreacted CO2 gas for cooling from 190°C to 175°C:

$$\dot{Q_2} = \dot{m} \times \int_{T_1}^{T} C_p(T)\, dT \tag{C.2}$$

$$\dot{Q_2} = 0.35 \times 469.5 \frac{kmol}{h} \times -159.683 \frac{cal}{mol} \times \frac{1h}{3600s} \times \frac{4.185J}{1cal} = -0.0305\text{MW}$$

The heat released from unreacted NH3 gas:

$$\dot{Q_3} = (792.9 + 191 - 2 \times 0.65 \times 469.5) \times \frac{kmol}{h} \times -143.545 \frac{cal}{mol} \times \frac{1h}{3600s} \times \frac{4.185J}{1cal} = -0.0024\text{MW}$$

The heat released from unreacted NH3 liquid:

$$\dot{Q_4} = 133 \frac{kmol}{h} \times 98006297 \frac{J}{kmol} \times \frac{1h}{3600s} = -3.62065\text{MW}$$

The heat released from Ammonium Carbamate cooling:

$$\dot{Q_5} = 515.2 \frac{kmol}{h} \times 2.59 \frac{kJ}{kgK} \times -15K \times 78.07 \frac{kg}{kmol} \times \frac{1h}{3600s} = -0.434\text{MW}$$

The net energy of the Carbamate Condenser:

$$\dot{Q}_{\text{condenser}} = \dot{Q}_1 + \dot{Q}_2 + \dot{Q}_3 + \dot{Q}_4 + \dot{Q}_5 \tag{C.3}$$

$$\dot{Q}_{\text{condenser}} = -7.123 + (-0.0305) + (-0.0024) + (-3.62065) + (-0.434) = -11.21MW$$

C.2 Calculations

Pressure at tube side changes from 9 to 4.5 bar at a constant temperature 147°C:
$\Delta H = 2119.71 - 2029.49 = 90.22kJ/kg$
Cooling water flow:

$$\dot{m} = \frac{11.21MW}{90.22kJ/kg} = 124kg/s$$

Tube-Side Coefficient

Water temperature (constant) = 147°C
Tube cross-sectional area:

$$A_t = \frac{25^2\pi}{4} = 490.87 \text{ mm}^2$$

Tubes per pass:

$$N_p = \frac{1116}{2} = 558$$

Total flow area:

$$A_f = 558 \times 490.87 \times 10^{-6} = 0.274 \text{ m}^2$$

Water mass velocity:

$$\dot{m}_w = \frac{124}{0.274} = 1651.66 \text{ kg/s} * \text{m}^2$$

Shell-Side Coefficient

Baffle spacing $= \frac{D_s}{5} = \frac{1147}{5} = 230$ mm
Tube pitch $= 1.25 \times 25 = 31.25$ mm
Cross-flow area:

$$A_s = \frac{(31.25 - 25)}{31.25} \cdot 1147 \cdot 230 \cdot 10^{-6} = 0.066 \text{ m}^2$$

Total input mass flowrate:

$$G_s = \frac{15.58kg/s}{0.066m^2} = 236 \text{ kg/sm}^2$$

Equivalent diameter:

$$d_e = \frac{1.1}{d_o}\left(\rho_t^2 - 0.917 \times d_0^{22}\right) = 17.75 \text{ mm}$$

Mean shell side temperature $= 182.5°\text{C}$
Average density $= 259 \text{ kg/m}^3$
Average viscosity $= 0.047cP$
Average heat capacity $= 1.657 \text{ kJ/kg}^\circ\text{C}$
Average thermal conductivity $= 0.192 \text{ W/m}^\circ\text{C}$

Overall Coefficient

$$\frac{1}{U} = \frac{1}{9307.4} + \frac{1}{5000} + \frac{0.025ln(0.025/0.0229)}{2 \times 16} + \frac{0.025}{0.0229} \times \frac{1}{3000} + \frac{0.025}{0.0229} \times \frac{1}{3418.7}$$

$$U = 944W/m^2C$$

Aspen Validation

Heat duty(calculated)=-11.21 MW Heat duty(Aspen)=-11.71 MW

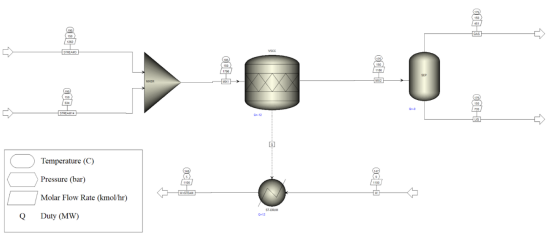

(a)

Outlet temperature	175	C
Outlet pressure	150	bar
Heat duty	-11.7136	MW
Net heat duty	-11.7136	MW
Vapor fraction	0.380662	
1st liquid / Total liquid	1	

(b)

Figure C.1: (a) Screenshot from the Aspen flowshee (b) Aspen duties

Appendix D

Evaporator Design Calculations

D.1 Required energy calculations:

The energy rate required to heat up a material, $\dot{Q}$ is simply given by

$$\dot{Q} = \dot{m} C_p \Delta T \tag{D.1}$$

Where $\dot{m}$ is the mass flow C_p is the specific heat of the material, and ΔT is the temperature change.
For the temp change from 80 °C to 100 °C: C_p of the liquid mixture is given by $\sum X_i C_{pi}$, where i is the component.

$$C_p = 46.812 + 37.735 + 0.1313 = 84.678 \frac{kJ}{kmol.K} \tag{D.2}$$

The energy required for T change from 80 °C to 100 °C:

$$\dot{Q}_1 = \dot{m} C_p T = 855.15 \times 84.678 \times 20 = 1448253 \frac{kJ}{h} \tag{D.3}$$

Energy for water vaporization, $\dot{Q}_v$ is

$$\dot{Q}_v = \dot{m} C_v = 428.11 \times 40.65 \times 10^3 = 17402671 \frac{kJ}{h} \tag{D.4}$$

where C_v is the specific heat of vaporization of water. C_p of vapor-liquid mixture is

$$C_p = \sum X_i C_{pi} = 46.812 + 18.772 + 0.1313 = 65.715 \frac{kJ}{kmol.K} \tag{D.5}$$

The energy required for T change from 100°C to 110°C is

$$\dot{Q}_2 = \dot{m} C_p T = 855.15 \times 65.715 \times 10 = 561962 \frac{kJ}{h} \tag{D.6}$$

The total energy required is 19 412 886 kJ/h

D.2 Heat transfer area calculations:

Area of the heat-exchanger, A is given by

$$A = \frac{\dot{Q}}{U \times \Delta T_{lm}} \tag{D.7}$$

Where U is the overall heat transfer coefficient and ΔT_{lm} is log mean temperature.

$$\begin{aligned} \Delta T_{lm} &= \frac{T_2 - T_1}{ln(T_2/T_1)} \\ T_1 = T_{hotin} - T_{coldin} &= 160 - 80 = 80^{\circ}C \\ T_2 = T_{hotout} - T_{coldout} &= 120 - 110 = 10^{\circ}C \\ T_{LMTD} &= \frac{10 - 80}{ln(10/80)} = 33.66^{\circ}C \end{aligned} \tag{D.8}$$

The temperature correction factor is 1 for the one shell pass and one tube pass heat-exchanger.

$$A = \frac{1.94 \times 10^{10}}{3600 \times 1500 \times 33.66} = 106.8m^2 \tag{D.9}$$

Typical falling film evaporator characteristics:
According to Sinnott and Towler [9], evaporator ranges from 1 to 6 m in length; tube diameters (outer) from 2.5 to 7.5 cm and tube lengths from 75 to 200 cm.
Assume tubes with 5cm diameter and 150cm length.

$$A = \pi \times D \times L \times n \tag{D.10}$$

Where n is the number of tubes, D is tube diameter, and L is length.
The above equation for number of tubes yields:

$$n = \frac{106.8}{\pi \times 1.5 \times 5 \times 10^{-2}} = 454 \tag{D.11}$$

Appendix E

Minor Units Design

E.1 CO_2 Compressor

Adiabatic head for the compressor is calculated as follows [72]:

$$H_{ad} = RT_i \left(\frac{k}{k-1}\right) \left[\left(\frac{P_o}{P_i}\right)^{\left(\frac{k-1}{k}\right)} - 1\right] \tag{E.1}$$

H_{ad} - adiabatic head, Nm/kmol
R - gas constant, $R = 8.314$ J/molK
T_i - inlet temperature, $T_i = 300$ K

$$k = \frac{C_p}{C_v} = \frac{1.417}{0.866} = 1.64 \tag{E.2}$$

$P_{i'} P_0 -$ inlet and outlet pressures, bar

The adiabatic head is:

$$H_{ad} = 8.314 \cdot 300 \cdot \left(\frac{1.64}{1.64-1}\right) \cdot \left[\left(\frac{150}{60}\right)^{\left(\frac{1.64-1}{1.64}\right)} - 1\right] = 2747.4 \text{ N m/kmol} \tag{E.3}$$

And the adiabatic power of the compression process is:

$$P_{ad} = \dot{F}_{CO_2} \cdot H_{ad} = 477 \frac{kmol}{hr} \cdot 2747.4 \frac{Nm}{kmol} \cdot \frac{1hr}{3600s} = 0.364 \text{ kW} \tag{E.4}$$

The adiabatic discharge temperature of CO2 is:

$$T_o = T_i \cdot \left(\frac{P_o}{P_i}\right)^{\frac{k-1}{k}} \tag{E.5}$$

$$T_o = 300 \cdot \left(\frac{150}{60}\right)^{\frac{1.64-1}{1.64}} = 430 \text{ K} \tag{E.6}$$

Ammonia Inlet Heat exchanger design:

Inlet flow rate of liquid NH_3 is 961.5 kmol/h = 16345.5 kg/h
Temperature change is from 27 °C to 190 °C
Heat capacity = 2.2 kJ/kg K

$$A = \frac{\dot{Q}}{U \times T_{LMTD}}$$
$$\dot{Q} = 16345.5 \times 2.2 \times (190 - 27) = 5.86 \times 106 = 1628kW$$
$$T_{LMTD} = (10 - 73)/ln(10/73) = 31.69$$

One shell and two tube passes:

$$R = \frac{200 - 100}{190 - 27} = 0.61$$
$$S = \frac{190 - 100}{200 - 27} = 0.52$$

Accoridng to Sinnott&Towel [9], $F_t = 0.93$

$$\Delta T_m = 0.93x31.69 = 29.5°C \tag{E.7}$$

Area calculations:

According to Luo et al.[73], the overall heat coefficient on ammonia is about $2000W/m^2K$.
$A = 1628 \times 10^3/(2000 \times 20.33) = 40.04m^2$
As [9] suggest, we take 20 mm outside diameter, 16 mm inside, 4.88 m length Copper - Brass tubes.
Assuming tube-sheet thickness, the length is 4.83m.
Area of one tube = $4.83 \times \pi \times 20 \times 10^{-3} = 0.304m^2$
Number of tubes = $40.04/0.304 = 132$
When considering the clean shell-side fluid, it's advisable to use a 1.25 triangular pitch for the tube arrangement.
Bundle diameter:

$$D_b = 20(\frac{132}{0.249})^{1/2.207} = 343mm$$

Suggested by Sinnott and Towler [9], the diametrical clearance for 1.25 triangular pitch bundle is 68 mm. So the shell diameter is *343+68=411mm*.

Tube side coefficient:

Mean temperature $= (27 + 190)/2 = 108.5°C$
Tube cross-sectional area $= \frac{\pi}{4}16^2 = 201.1mm$
Tubes per pass $= 132/2 = 66$
Total flow area $= 66 \times 201 \times 10^{-6} = 0.013m^2$
Ammonia mass velocity $= 4.54/0.013 = 349kg/sm^2$ According to [74], ammonia density is

$$\rho = \frac{P}{0.6(T_F + 460)} \tag{E.8}$$

Where P is the absolute pressure in psia and T_F temperature in °F.

$$\rho = \frac{2176}{0.6(374 + 460)} = 4.34lb/ft^3 = 69.52kg/m^3$$

Thermal conductivity = 67.9 mW/m.K
Specific heat = $C_p = 0.393 + 0.00037_k(cal/g°C)$
$C_p = 0.53(cal/g°C)) = 2.22(kJ/kg.K)$
Ammonia linear velocity = 349/69.52 = 5.02 m/s
Ammonia viscosity[75] = 242.30 microP.s

$$Re = \frac{\rho \times u \times d_i}{\mu} = \frac{880 \times 5.02 \times 16 \times 10^{-3}}{242.30 \times 10^{-6}} = 2.9 \times 10^5$$

$$Pr = \frac{C_p\mu}{k} = \frac{0.53 \times 4.184 \times 18.72 \times 10^{-3}}{67.9x10^{-3}} = 0.61$$

$$\frac{L}{d_i} = \frac{4.83 \times 10^3}{16}$$

The formula to calculate the heat coefficient is given in equation **??**.
The j_h = is measured from the plot in figure **??** and is equal t $2.5x10^{-3}$.
According to [9], viscosity correction factor can be ignored for similar viscosity fluids.

$$h = 67.9 \times 10^{-3}/(16 \times 10^{-3} \times 2.5 \times 10^{-3} \times 291711 \times 0.61^{0.33} = 2617W/m2K$$

Shell side coefficient:

Standard baffle spacing = 411/5 =82 mm
Tube pitch = 1.25*20 = 25 mm

Cross flow area = (25-20)/25x411x82x10^{-6}=0.007 m^2
Steam mass flow rate for the given $\dot{Q}$ and ΔT:
1628/(2.00x100)=8.14 kg/s
Mass velocity = 8.14/0.007= 1163 kg/s m^2
Equivalent diameter = 14.4 mm
Mean shell side temperature = (100+200)/2=150 °C
Steam pressure is 100 bar[76].
Steam at 200 C and 100 bar is water and its density is [77] = 871 kg/m3
Viscosity[77]= 1.367e-4 Pa.s
Specific heat capacity Cp= 4.45 kJ/kg.K
Thermal conductivity at 100 bar and 200 C [78]: k = 668 mW/m.K
$Re = 1163 * 14.4 * 10^{-3}/1.367 * 10^{-4} = 1.2 * 10^5$
$Pr = 4.45 * 10^3 * 1.367x10^{-4}/0.668 = 0.91$
Using 25% baffle cut[9], the j_h is 1.5×10^{-3}
Viscosity correction factor is ignored.
$h_s = 0.668 * 1.5 * 10^{-3} * 1.2 * 10^5 * 0.94^{0.33}/(14.4 * 10^{-3}) = 8146 W/m^2K$

Overall coefficient:

$$\frac{1}{U} = \frac{1}{h_i} + \frac{L}{k} + \frac{1}{h_o}$$

Where k is the heat conductivity of Copper - Brass tubes given by 111 W/m.K.

$$\frac{1}{U} = \frac{1}{8146} + \frac{2x10^{-3}}{111} + \frac{1}{2617}$$

So U is 1912 W/m^2K.

The consistency between the assumed and calculated overall heat transfer coefficients validates the accuracy of the initial design assumptions and confirms the robustness of the heat transfer analysis conducted. It suggests that the selected specifications are well-aligned with the operational requirements.

E.2 Low Pressure Absorber

In low pressure absorber NH3 and CO2 separated from the urea solution in low pressure decomposer are recovered. Heat released from that reaction is used to

produce steam at 2 bar. This steam is used for the evaporation process of the lower and upper separator.
Net heat duty of LP Absorber:

$$\dot{Q} = -3.98MW$$

Logmean temperature difference:

$$\Delta T_{lm} = 18.7C$$

Taking the correction factor as 0.8:

$$\Delta T_{lm} = 18.7 \times 0.8 = 14.96C$$

Heat transfer area was calculated as follows (taking the same heat transfer coefficient as for the condenser):

$$A = \frac{3.98MW}{750W/(m^{2*}C) * 14.96C} = 354.7 \text{ m}^2 \tag{E.9}$$

The number of tubes in the heat exchanger was calculated with the following equation:

$$N = \frac{354.7 \text{ m}^2}{\pi^* 0.025 \text{ m}^* 6.1 \text{ m}} = 740 \tag{E.10}$$

Then, the tube bundle diameter with square pitch and one pass.

$$D_b = 0.025m \times (740/0.215)^{1/2.207} = 1001mm \tag{E.11}$$

Cooling water requirement:

$$m_w = \frac{3.98 * 10^6}{4200 \times 30} = 31.58 \text{ kg/s} \tag{E.12}$$

E.3 Middle Pressure Absorber

In the middle pressure absorber NH3 and CO2 separated from the urea solution in medium pressure decomposer are recovered. Condensation heat in the middle

pressure absorber is transferred directly to the aqueous urea solution feed in the final concentration section. Heat released from MP Absorber:

$$\dot{Q}_1 = -3.63MW$$

The heat required to heat output from Low Pressure Decomposer:

$$\dot{Q}_2 = 0.44MW$$

Net heat duty of MP Absorber:

$$\dot{Q} = \dot{Q}_1 + \dot{Q}_2 = 3.19MW$$

Logmean temperature difference:

$$\Delta T_{lm} = 28.93C$$

Taking the correction factor as 0.8:

$$\Delta T_{lm} = 28.93 \times 0.8 = 23.14C$$

Heat transfer area was calculated as follows (taking the same heat transfer coefficient as for the condenser):

$$A = \frac{3.19MW}{750W/(m^{2*}C) * 23.14C} = 183.8\ \mathrm{m}^2 \tag{E.13}$$

The number of tubes in the heat exchanger was calculated with the following equation:

$$N = \frac{183.8\ \mathrm{m}^2}{\pi^{*}0.025\ \mathrm{m}^{*}6.1\ \mathrm{m}} = 384 \tag{E.14}$$

Then, the tube bundle diameter with square pitch and one pass.

$$D_b = 0.025m \times (384/0.215)^{1/2.207} = 744mm \tag{E.15}$$

Cooling water requirement:

$$m_w = \frac{3.19 * 10^6}{4200 \times (70 - 30)} = 18.93\ \mathrm{kg/s} \tag{E.16}$$

E.4 Middle Pressure Decomposer

Middle Pressure Decomposer is a falling-film heat exchanger [source]. It consists of tubes, where the mixture of urea, water and biuret and ammonium carbamate flows downward along tube walls, while carbon dioxide and ammonia from decomposed ammonium carbamate rises upward. The heat requirements for this unit is equal to 10.87 MW. The mean temperature is calculated below:

$$\Delta T_{lm} = \frac{195degC - 150degC}{\ln\left((225degC - 195degC) \,/\, (225degC - 150degC)\right)} = 49.11 \deg C \quad \text{(E.17)}$$

Heat transfer area was calculated as the following (taking the same heat transfer coefficient as for the stripper:

$$A = \frac{10.87\text{MW}}{750 \text{ W}/ (\text{m}^{2*} \text{ K}) * 49.11\text{degC}} = 295 \text{ m}^2 \quad \text{(E.18)}$$

The number of tubes in the heat exchanger was calculated with the following equation (the tube pitch, length and diameter were the same as for the stripper):

$$N = \frac{A}{\pi^* OD_t^* L} = \frac{295 \text{ m}^2}{\pi^* 0.031 \text{ m}^* 6 \text{ m}} = 505$$

Then, the following equation was used to calculate tube bundle diameter with square pitch and one pass.

$$D_b = OD_t \left(N_t / K_1\right)^{1/n1} = 0.031m \times (505/0.215)^{1/2.207} = 1044mm \quad \text{(E.19)}$$

The following equation demonstrates calculation of steam requirement.

$$m_s = \frac{Q}{\Delta H} = \frac{10.87KW}{1834.25 \text{ kJ/kg}} = 5.90kg/s \quad \text{(E.20)}$$

E.5 Low Pressure Decomposer

Low Pressure Decomposer is also a falling-film heat exchanger [source]. The heat requirements for this unit is equal to 25MW. The mean temperature is calculated below:

$$\Delta T_{lm} = \frac{70\,\text{deg}\,C - 80\,\text{deg}\,C}{\ln((225\,\text{deg}\,C - 80\,\text{deg}\,C)/(225\,\text{deg}\,C - 70\,\text{deg}\,C))} = 149.9\,\text{deg}\,C \quad \text{(E.21)}$$

Heat transfer area was calculated as the following (taking the same heat transfer coefficient as for the stripper):

$$A = \frac{25MW}{750W/(m^{2*}K) * 149.9degC} = 222\ \text{m}^2 \quad \text{(E.22)}$$

The number of tubes in the heat exchanger was calculated with the following equation:

$$N = \frac{A}{\pi^* OD_t^* L} = \frac{222\ \text{m}^2}{\pi^* 0.031\ \text{m}^* 6\ \text{m}} = 381 \quad \text{(E.23)}$$

Then, the following equation was used to calculate tube bundle diameter with square pitch and one pass.

$$D_b = OD_t\,(N_t/K_1)^{1/n1} = 0.031m \times (381/0.215)^{1/2.207} = 919mm \quad \text{(E.24)}$$

Low pressure steam requirement was calculated with the following formula:

$$m_s = \frac{Q}{\Delta H} = \frac{25\text{MW}}{1834.25\ \text{kJ/kg}} = 13.63\ \text{kg/s} \quad \text{(E.25)}$$

E.6 Warehouse Urea Bags Storage

Based on the bulk density of the urea, which is 0.8 tonnes per meter cubed [56], and volume of 1 bag, which is 1 meter cubed, number of bags is:

$$\frac{600tm^3 \times 7d \times 1bag}{d \times 0.8t \times 1w \times 1m^3} = 5250bags \quad \text{(E.26)}$$

3 bags are to be placed over one another (5250 / 3 = 1750 rows of bags, 3 bags in each raw), there are 5 raws of bags, 1 raw containing 2 bags close to each other (5 rows with 2 bags = 10, 1750 / 10 = 175 in 1 line)

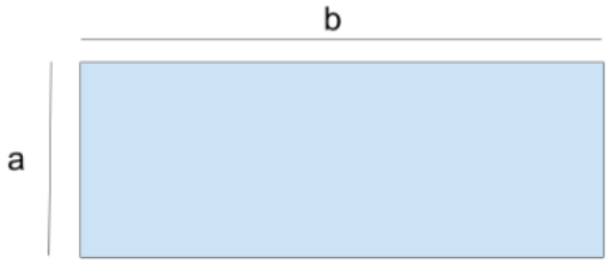

Figure E.1: The dimensions of the urea bags storage, view from above

For a: 5 rows with 2 bags, 10 m + space between them of 3 bags, 4 spaces, 12 m 22 m.

For b: bag to bag, almost no space between them, 175m + space before the doors approx. 3 bags to each end 6 m, together 181 m.

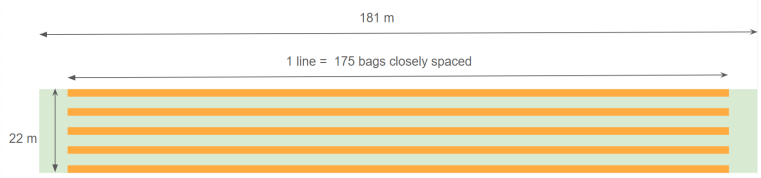

Figure E.2: The schematics with right aspect ratio of the warehouse prilled urea bags storage, green representing the empty space and orange representing the bags.

Appendix F

Cost Estimations

F.1 Installed cost calculations

$$C_{installed} = C_{equipment}((1 + f_p) \times f_m + (f_{er} + f_{el} + f_i + f_c + f_s + f_l))$$

Factor	Coefficient
fm	1.5
fer	0.3
fp	0.8
fi	0.3
fel	0.2
fc	0.3
fs	0.2
fl	0.1

Table F.1: Coefficients for Calculation of Installed Cost